

Non-decoupling SUSY in LFV Higgs decays: a window to new physics at the LHC

M. ARANA-CATANIA^{1*}, E. ARGANDA^{2†}, M.J. HERRERO^{1‡}

¹*Departamento de Física Teórica and Instituto de Física Teórica, IFT-UAM/CSIC
Universidad Autónoma de Madrid, Cantoblanco, Madrid, Spain*

²*IFLP, CONICET - Dpto. de Física, Universidad Nacional de La Plata,
C.C. 67, 1900 La Plata, Argentina*

Abstract

The recent discovery of a SM-like Higgs boson at the LHC, with a mass around 125-126 GeV, together with the absence of results in the direct searches for supersymmetry, is pushing the SUSY scale (m_{SUSY}) into the multi-TeV range. This discouraging situation from a low-energy SUSY point of view has its counterpart in indirect SUSY observables which present a non-decoupling behavior with m_{SUSY} . This is the case of the one-loop lepton flavor violating Higgs decay rates induced by SUSY, which are shown here to remain constant as m_{SUSY} grows, for large $m_{\text{SUSY}} > 2$ TeV values and for all classes of intergenerational mixing in the slepton sector, LL , LR , RL and RR . In this work we focus on the LFV decays of the three neutral MSSM Higgs bosons h , H , $A \rightarrow \tau\mu$, considering the four types of slepton mixing (δ_{23}^{LL} , δ_{23}^{LR} , δ_{23}^{RL} , δ_{23}^{RR}), and show that all the three channels could be measurable at the LHC, being $h \rightarrow \tau\mu$ the most promising one, with up to about hundred of events expected with the current LHC center-of-mass energy and luminosity. The most promising predictions for the future LHC stage are also included.

*email: miguel.arana@uam.es

†email: ernesto.arganda@fisica.unlp.edu.ar

‡email: maria.herrero@uam.es

1 Introduction

The absence of any experimental signal, so far, in the searches for supersymmetry (SUSY) at the LHC [1] and the discovery of a new Higgs-like particle by ATLAS [2] and CMS [3] with a mass $m_{H_{\text{SM}}} \simeq 125\text{-}126$ GeV, are pushing the SUSY mass parameters above the 1-TeV range. On one hand, the present lower mass bounds for squarks of the first and second generations and for gluinos are already above 1 TeV, and on the other hand, if the observed Higgs boson is identified with the lightest Higgs boson h of the Minimal Supersymmetric Standard Model (MSSM), a radiatively corrected mass $m_h \simeq 125\text{-}126$ GeV also implies rather heavy squark masses of the third generation (mainly stop masses) at or larger than 1 TeV. In principle, to place the SUSY masses at the multi-TeV range seems discouraging, both from an experimental point of view due to the inability to detect SUSY directly, and from a theoretical point of view, in regard to the naturalness of the theory, which contrarily suggests a soft SUSY-breaking scale, m_{SUSY} , at or below the TeV scale. However, leaving the naturalness issue aside, the MSSM scenarios with very heavy SUSY masses can have other interesting aspects [4]. In particular, this is the case of specific Higgs boson observables, like certain Higgs partial decay widths, which present a non-decoupling behavior with m_{SUSY} , as shown, for instance, in [5–9], opening a new window to the indirect detection of heavy SUSY. As it is well known, the decoupling of SUSY radiative corrections in the asymptotic large SUSY mass limit is valid for SUSY theories with an exact gauge symmetry, in agreement with the general decoupling behavior of heavy states in Quantum Field Theory as stated in the famous Appelquist-Carazzone theorem [10]. Nevertheless, it is also known that this theorem does not apply to theories with spontaneously broken gauge symmetries, nor with chiral fermions, which is the case of the MSSM. Furthermore, in order to have decoupling, the dimensionless couplings should not grow with the heavy masses. Otherwise, the mass suppression induced by the heavy-particle propagators can be compensated by the mass enhancement provided by the interaction vertices, with an overall non-decoupling effect, which is exactly what happens in some MSSM Higgs boson decays to fermions. For instance, it was studied in [5] how non decoupling appears for large SUSY masses in the $h \rightarrow b\bar{b}$ decay through one-loop SUSY-QCD corrections, when the involved SUSY particle masses grow simultaneously with a generic soft SUSY-breaking scale m_{SUSY} (see also [6]). A similar non-decoupling behavior was obtained for flavor changing neutral Higgs boson decays into quarks of the second and third generations through both SUSY-QCD corrections [7] and SUSY-EW corrections [8]. Other interesting non-decoupling SUSY-EW effects have also been seen in lepton flavor violating (LFV) Higgs boson decays within the context of the MSSM-seesaw model [9]; and in Higgs-mediated LFV processes like: $\tau \rightarrow 3\mu$ decays [11], some semileptonic τ decays [12, 13] and in $\mu - e$ conversion in heavy nuclei [14]; all of them within the MSSM-seesaw model too. Other non-decoupling effects from heavy SUSY particles have also been noticed within the context of the SUSY inverse-seesaw model [15]. Some studies of SUSY non decoupling within the MSSM have also been performed in the effective field theory approach where the effective Higgs-fermion-fermion vertices are induced from one-loop corrections of heavy SUSY particles [6, 16] and in $b\bar{b}h$ production [17].

In the present work, motivated by the recent discovery of the SM-like Higgs boson, we will focus on the study of the LFV Higgs boson decays and we will work within the context of the MSSM at one-loop order with the hypothesis of general slepton flavor mixing. We will extend the study to the three neutral Higgs bosons of the MSSM h , H and A , considering the new Higgs-like particle to be the lightest Higgs boson h . In particular, we will study the LFV Higgs decays $h \rightarrow \tau\mu$, $H \rightarrow \tau\mu$ and $A \rightarrow \tau\mu$. This kind of processes provide an unique window into new physics due to the strong suppression of flavor violation in the Standard Model (SM), where the flavor mixing is induced exclusively by the Yukawa couplings of the corresponding fermion sector. This is specially

interesting in the lepton sector in which the flavor mixing will be hugely suppressed because of the smallness of the lepton Yukawa couplings. Therefore, the discovery of any process which violates the lepton flavor number would be a clear signal of physics beyond the SM. LFV is nowadays a very active field which is being studied in different models, through several channels (for a review, see for instance [18]): radiative decays $\tau \rightarrow \mu\gamma$, $\tau \rightarrow e\gamma$ and $\mu \rightarrow e\gamma$; 3-body decays $\tau \rightarrow 3\mu$, $\tau \rightarrow 3e$ and $\mu \rightarrow 3e$; $\mu - e$ conversion in nuclei; semileptonic τ decays; among others. The specific case of LFV Higgs decays within supersymmetric models has also deserved special attention in the literature [9, 19]. Also encouraging results for the reach of LFV Higgs decays at the LHC have been recently obtained in [20] within the context of a general effective Lagrangian approach.

Our purpose here is to take advantage of the mentioned non-decoupling behavior with m_{SUSY} in the LFV Higgs decay widths into charged leptons of different generations, $\Gamma(\phi \rightarrow l_i l_j)$, with $i \neq j$ and $\phi = h, H, A$, in order to look for sizeable branching ratios which can give rise to detectable signals at the LHC. Here and from now on, $l_i l_j$ with $i \neq j$ in the final state of the LFV decays refers to either $l_i \bar{l}_j$ or $\bar{l}_i l_j$. In general, the radiatively corrected LFV Higgs couplings to leptons are proportional to the heaviest lepton mass involved, being this the reason why we select the $\tau\mu$ channel as the most promising one. In addition, the μe channel is extremely restricted by the associated radiative decay, $\mu \rightarrow e\gamma$ [21], leaving us almost no room to move in the allowed parameter space of slepton flavor mixing, and driving us to extremely low rates, not measurable in any LHC detector. The τe channel, on the other hand, gives us very similar results to the $\tau\mu$ channel, and from an experimental point of view, the LHC sensitivity to the former should be equivalent to the latter [22]. Therefore the results obtained along this work for the LFV Higgs decays into $\tau\mu$ are straightforwardly translated into the τe channels. For the present study we will focus then on the $\phi \rightarrow \tau\mu$ decays within the MSSM at one loop with general slepton flavor mixing between the second and the third generations, without assuming any particular source of flavor mixing. Consequently, this general slepton mixing will be parametrized in a model-independent way by four dimensionless parameters, δ_{23}^{LL} , δ_{23}^{LR} , δ_{23}^{RL} and δ_{23}^{RR} . It is important to remark that our calculations will be made in the mass eigenstate basis for all MSSM particles, including both charged sleptons and sneutrinos with the corresponding exact diagonalization of the full charged slepton and sneutrino mass matrices, and therefore we will not use here the Mass Insertion Approximation (MIA). The most important constraints to these four slepton mixings come from the $\tau \rightarrow \mu\gamma$ searches [23]. A recent study on updated constraints to all these general slepton flavor mixings δ_{ij}^{AB} in [24] indicates that, indeed, the present bounds to $\text{BR}(\tau \rightarrow \mu\gamma)$ lead to constraints on the 23 mixings which for $500 \text{ GeV} \leq m_{\text{SUSY}} \leq 1500 \text{ GeV}$ and $5 \leq \tan\beta \leq 60$ are at $|\delta_{23}^{LL}|_{\text{max}}, |\delta_{23}^{LR}|_{\text{max}}, |\delta_{23}^{RL}|_{\text{max}} \sim \mathcal{O}(10^{-2} - 10^{-1})$, and $|\delta_{23}^{RR}|_{\text{max}} \sim \mathcal{O}(10^{-1} - 1)$, and for heavier SUSY masses lead to weaker bounds. We will check that by raising the SUSY mass scale into the multi-TeV range will turn into the needed relaxation of these bounds, since these LFV radiative decays present a decoupling behavior with the SUSY scale. This will allow us to explore a high SUSY mass scale region, where we will find very promising values for the LFV Higgs rates.

Our paper is structured as follows: in Section 2 we describe the MSSM frame which we will use in the rest of the paper, introducing the flavor mixing and the scenarios we will work with. Section 3 is devoted to the LFV Higgs decay rates in the heavy SUSY particle mass limit, showing the non-decoupling behavior of these rates with m_{SUSY} . We dedicate Section 4 to the relevant numerical results of the LFV Higgs event rates at the LHC, considering the effects induced by each type of delta, δ_{23}^{AB} . This will be done taking into account the conditions of the present and future phases of the LHC, in order to estimate the number of events one could expect for each LFV Higgs channel. We will finally close the paper with the conclusions, contained in Section 5.

2 The MSSM with general slepton mixing

In this paper we explore SUSY scenarios with general flavor mixing in the slepton sector, which have the same particle content as the MSSM. Within these scenarios, the most general hypothesis of flavor mixing assumes a non-diagonal mass matrix in flavor space, for both charged slepton and sneutrino sectors. The charged slepton mass matrix is a 6×6 matrix due to the six electroweak interaction eigenstates, $\tilde{l}_{L,R}$ with $l = e, \mu, \tau$. The inclusion, within the MSSM, of only three sneutrino eigenstates, $\tilde{\nu}_L$ with $\nu = \nu_e, \nu_\mu, \nu_\tau$, reduces the sneutrino mass matrix to a 3×3 matrix. In the case in which slepton and sneutrino mass matrices were diagonal, we would still have a tiny flavor violation induced by the PMNS matrix of the neutrino sector and transmitted by the tiny neutrino Yukawa couplings, but we neglect it here.

The non-diagonal entries in the 6×6 slepton matrix can be described in a model-independent way in terms of a set of dimensionless parameters δ_{ij}^{AB} ($A, B = L, R; i, j = 1, 2, 3$), where L, R stand for the possible chiralities of the lepton partners and i, j indexes run over the three generations. These scenarios with general sfermion flavor mixing lead generally to larger LFV rates than in the so-called Minimal Flavor Violation (MFV) scenarios, where the mixing is induced exclusively by the Yukawa coupling of the corresponding fermion sector. This statement is true for both squarks and sleptons but it is obviously of special interest in the slepton case due to the extremely small size of the lepton Yukawa couplings. Hence, in the present case of slepton mixing, the δ_{ij}^{AB} 's will provide the unique origin of LFV processes with potentially measurable rates.

One usually starts with the non-diagonal 6×6 slepton squared mass matrix referred to the electroweak interaction basis, which we order here as $(\tilde{e}_L, \tilde{\mu}_L, \tilde{\tau}_L, \tilde{e}_R, \tilde{\mu}_R, \tilde{\tau}_R)$, and write this matrix in terms of left- and right-handed blocks M_{lAB}^2 ($A, B = L, R$), which are non-diagonal 3×3 matrices,

$$\mathcal{M}_l^2 = \begin{pmatrix} M_{lLL}^2 & M_{lLR}^2 \\ M_{lLR}^{2\dagger} & M_{lRR}^2 \end{pmatrix}, \quad (1)$$

where

$$\begin{aligned} M_{lLL}^2 &= m_{\tilde{L}}^2 + \left(m_{l_i}^2 + \left(-\frac{1}{2} + \sin^2 \theta_W \right) M_Z^2 \cos 2\beta \right) \delta_{ij}, \\ M_{lRR}^2 &= m_{\tilde{E}}^2 + (m_{l_i}^2 - \sin^2 \theta_W M_Z^2 \cos 2\beta) \delta_{ij}, \\ M_{lLR}^2 &= v_1 \mathcal{A}_{ij}^l - m_{l_i} \mu \tan \beta \delta_{ij}, \end{aligned} \quad (2)$$

with flavor indexes $i, j = 1, 2, 3$, corresponding to the first, second and third generations, respectively. θ_W is the weak angle, M_Z is the Z gauge boson mass, $(m_{l_1}, m_{l_2}, m_{l_3}) = (m_e, m_\mu, m_\tau)$ are the lepton masses, $\tan \beta = v_2/v_1$ with $v_1 = \langle \mathcal{H}_1^0 \rangle$ and $v_2 = \langle \mathcal{H}_2^0 \rangle$, the two vacuum expectation values of the corresponding neutral Higgs boson in the Higgs $SU(2)$ doublets, $\mathcal{H}_1 = (\mathcal{H}_1^0 \ \mathcal{H}_1^-)$ and $\mathcal{H}_2 = (\mathcal{H}_2^+ \ \mathcal{H}_2^0)$, and μ is the usual higgsino mass term. It should be noted that the non diagonality in flavor comes exclusively from the soft SUSY-breaking parameters, which could be non vanishing for $i \neq j$, namely: the masses $m_{\tilde{L}_{ij}}$ for the slepton $SU(2)$ doublets $(\tilde{\nu}_{Li} \ \tilde{l}_{Li})$, the masses $m_{\tilde{E}_{ij}}$ for the slepton $SU(2)$ singlets (\tilde{l}_{Ri}) , and the trilinear couplings, \mathcal{A}_{ij}^l .

In the sneutrino sector there is, correspondingly, a one-block 3×3 mass matrix, respect to the $(\tilde{\nu}_{eL}, \tilde{\nu}_{\mu L}, \tilde{\nu}_{\tau L})$ electroweak interaction basis,

$$\mathcal{M}_\nu^2 = (\ M_{\nu LL}^2 \), \quad (3)$$

where

$$M_{\nu LL}^2 = m_{\tilde{L}}^2 + \left(\frac{1}{2} M_Z^2 \cos 2\beta \right) \delta_{ij}. \quad (4)$$

It should be also noted that, due to $SU(2)_L$ gauge invariance, the same soft masses $m_{\tilde{L}ij}$ enter in both the slepton and sneutrino LL mass matrices. Besides, in the previous equations we have neglected the neutrino mass terms, which due to their extremely small value are totally irrelevant for the present computation.

The general slepton flavor mixing is then introduced via the non-diagonal terms in the soft-breaking slepton mass matrices and trilinear coupling matrices, which are defined here as

$$m_{\tilde{L}}^2 = \begin{pmatrix} m_{\tilde{L}_1}^2 & \delta_{12}^{LL} m_{\tilde{L}_1} m_{\tilde{L}_2} & \delta_{13}^{LL} m_{\tilde{L}_1} m_{\tilde{L}_3} \\ \delta_{21}^{LL} m_{\tilde{L}_2} m_{\tilde{L}_1} & m_{\tilde{L}_2}^2 & \delta_{23}^{LL} m_{\tilde{L}_2} m_{\tilde{L}_3} \\ \delta_{31}^{LL} m_{\tilde{L}_3} m_{\tilde{L}_1} & \delta_{32}^{LL} m_{\tilde{L}_3} m_{\tilde{L}_2} & m_{\tilde{L}_3}^2 \end{pmatrix}, \quad (5)$$

$$v_1 \mathcal{A}^l = \begin{pmatrix} m_e A_e & \delta_{12}^{LR} m_{\tilde{L}_1} m_{\tilde{E}_2} & \delta_{13}^{LR} m_{\tilde{L}_1} m_{\tilde{E}_3} \\ \delta_{21}^{LR} m_{\tilde{L}_2} m_{\tilde{E}_1} & m_\mu A_\mu & \delta_{23}^{LR} m_{\tilde{L}_2} m_{\tilde{E}_3} \\ \delta_{31}^{LR} m_{\tilde{L}_3} m_{\tilde{E}_1} & \delta_{32}^{LR} m_{\tilde{L}_3} m_{\tilde{E}_2} & m_\tau A_\tau \end{pmatrix}, \quad (6)$$

$$m_{\tilde{E}}^2 = \begin{pmatrix} m_{\tilde{E}_1}^2 & \delta_{12}^{RR} m_{\tilde{E}_1} m_{\tilde{E}_2} & \delta_{13}^{RR} m_{\tilde{E}_1} m_{\tilde{E}_3} \\ \delta_{21}^{RR} m_{\tilde{E}_2} m_{\tilde{E}_1} & m_{\tilde{E}_2}^2 & \delta_{23}^{RR} m_{\tilde{E}_2} m_{\tilde{E}_3} \\ \delta_{31}^{RR} m_{\tilde{E}_3} m_{\tilde{E}_1} & \delta_{32}^{RR} m_{\tilde{E}_3} m_{\tilde{E}_2} & m_{\tilde{E}_3}^2 \end{pmatrix}. \quad (7)$$

In all this work, for simplicity, we are assuming that all δ_{ij}^{AB} parameters are real. Therefore, hermiticity of \mathcal{M}_l^2 and \mathcal{M}_ν^2 implies $\delta_{ij}^{AB} = \delta_{ji}^{BA}$. Besides, in order to avoid extremely large off-diagonal matrix entries we restrict ourselves to $|\delta_{ij}^{AB}| \leq 1$. It is worth to have in mind for the rest of this work that our parametrization of the off-diagonal in flavor space entries in the above mass matrices is purely phenomenological and does not rely on any specific assumption about the origin of the MSSM soft-mass parameters. In particular, it should be noted that our parametrization for the LR and RL squared mass entries connecting different generations (i.e. for $i \neq j$) assumes a similar generic form to the LL and RR entries. For instance, $M_{lLR23}^2 = \delta_{23}^{LR} m_{\tilde{L}_2} m_{\tilde{E}_3}$. This implies that our hypothesis for the trilinear off-diagonal couplings \mathcal{A}_{ij}^l with $i \neq j$ (as derived from Eq.(6)) is one among other possible definitions considered in the literature. In particular, it is related to the usual assumption $M_{lLRij}^2 \sim v_1 m_{\text{SUSY}}$, by setting $\mathcal{A}_{ij}^l \sim \mathcal{O}(m_{\text{SUSY}})$. Here, $v_1^2 + v_2^2 = v^2 = 2 \frac{M_W^2}{g^2}$, M_W is the charged gauge boson mass, g is the $SU(2)_L$ gauge coupling and m_{SUSY} is a typical SUSY mass scale. It should be also noted that the diagonal entries in Eq.(6) have been normalized as it is usual in the literature, namely, by factorizing out the corresponding lepton Yukawa coupling: $\mathcal{A}_{ii}^l = y_i A_{ii}^l$, with $A_{11}^l = A_e$, $A_{22}^l = A_\mu$ and $A_{33}^l = A_\tau$. Finally, it should be mentioned that our choice in Eqs.(5), (6) and (7) is to normalize the non-diagonal in flavor entries with respect to the geometric mean of the corresponding diagonal squared soft masses. For instance,

$$\begin{aligned} \delta_{23}^{LL} &= (m_{\tilde{L}}^2)_{23}/(m_{\tilde{L}_2} m_{\tilde{L}_3}), & \delta_{23}^{RR} &= (m_{\tilde{R}}^2)_{23}/(m_{\tilde{R}_2} m_{\tilde{R}_3}), \\ \delta_{23}^{LR} &= (v_1 \mathcal{A}^l)_{23}/(m_{\tilde{L}_2} m_{\tilde{R}_3}), & \delta_{32}^{RL} &= \delta_{32}^{LR} = (v_1 \mathcal{A}^l)_{32}/(m_{\tilde{L}_3} m_{\tilde{R}_2}). \end{aligned} \quad (8)$$

The next step is to rotate the sleptons and sneutrinos from the electroweak interaction basis to the physical mass eigenstate basis,

$$\begin{pmatrix} \tilde{l}_1 \\ \tilde{l}_2 \\ \tilde{l}_3 \\ \tilde{l}_4 \\ \tilde{l}_5 \\ \tilde{l}_6 \end{pmatrix} = R^{\tilde{l}} \begin{pmatrix} \tilde{e}_L \\ \tilde{\mu}_L \\ \tilde{\tau}_L \\ \tilde{e}_R \\ \tilde{\mu}_R \\ \tilde{\tau}_R \end{pmatrix}, \quad \begin{pmatrix} \tilde{\nu}_1 \\ \tilde{\nu}_2 \\ \tilde{\nu}_3 \end{pmatrix} = R^{\tilde{\nu}} \begin{pmatrix} \tilde{\nu}_{eL} \\ \tilde{\nu}_{\mu L} \\ \tilde{\nu}_{\tau L} \end{pmatrix}, \quad (9)$$

with $R^{\tilde{l}}$ and $R^{\tilde{\nu}}$ being the respective 6×6 and 3×3 unitary rotating matrices which yield the diagonal mass-squared matrices as follows,

$$\text{diag}\{m_{\tilde{l}_1}^2, m_{\tilde{l}_2}^2, m_{\tilde{l}_3}^2, m_{\tilde{l}_4}^2, m_{\tilde{l}_5}^2, m_{\tilde{l}_6}^2\} = R^{\tilde{l}} \mathcal{M}_{\tilde{l}}^2 R^{\tilde{l}\dagger}, \quad (10)$$

$$\text{diag}\{m_{\tilde{\nu}_1}^2, m_{\tilde{\nu}_2}^2, m_{\tilde{\nu}_3}^2\} = R^{\tilde{\nu}} \mathcal{M}_{\tilde{\nu}}^2 R^{\tilde{\nu}\dagger}. \quad (11)$$

In the numerical computations of the present study we will restrict ourselves to the case where there are flavor mixings exclusively between the second and third generations of sleptons, thus we set all δ_{ij}^{AB} 's to zero except for $ij = 23$. On one hand, the LFV one-loop corrected Higgs couplings are proportional to the heaviest lepton mass involved [9] and, therefore, the Higgs decay rates into μe are suppressed by a factor m_μ^2/m_τ^2 with respect to the $h, H, A \rightarrow \tau\mu, \tau e$ decay rates. On the other hand, the related LFV radiative decay $\mu \rightarrow e\gamma$ has a much more restrictive upper bound [21] than $\tau \rightarrow e\gamma$ and $\tau \rightarrow \mu\gamma$ decays [23], and the present allowed values of the δ_{12}^{AB} 's would not drive us to any measurable $\phi \rightarrow \mu e$ rates.

In order to simplify our analysis, and to reduce further the number of independent parameters, we will focus on the following numerical study on simplified SUSY scenarios, where the relevant soft-mass parameters are related to a single SUSY mass scale, m_{SUSY} . In particular we choose the following setting for the relevant mass parameters:

$$m_{\tilde{L}} = m_{\tilde{E}} = m_{\text{SUSY}}, \quad (12)$$

$$\mu = M_2 = a m_{\text{SUSY}}, \quad (13)$$

where a is a constant coefficient that we will fix in the next sections to different values, namely, $a = \frac{1}{5}, \frac{1}{3}, 1$. We also set an approximate GUT relation for the gaugino masses:

$$M_2 = 2M_1 = M_3/4. \quad (14)$$

Here and in the following we use a short notation for the common soft masses, namely, $m_{\tilde{L}}$ for $m_{\tilde{L}} = m_{\tilde{L}_1} = m_{\tilde{L}_2} = m_{\tilde{L}_3}$, etc. For simplicity, we have also assumed vanishing soft-trilinear couplings for the first and second generations in the slepton sector, i.e., $A_\mu = A_e = 0$. We have checked that other choices with non-vanishing values for any of these two couplings do not alter the conclusions of this work. The trilinear coupling for the third generation has been fixed here to the generic SUSY mass scale, $A_\tau = m_{\text{SUSY}}$.

Regarding the non-diagonal trilinear couplings we have also assumed a rather simple but realistic setting by relating them with the single soft SUSY-breaking mass scale, m_{SUSY} . Specifically, we assume the following linear relation:

$$\mathcal{A}_{23}^l = \tilde{\delta}_{23}^{LR} m_{\text{SUSY}}, \quad \mathcal{A}_{32}^l = \tilde{\delta}_{32}^{LR} m_{\text{SUSY}}, \quad (15)$$

where the new dimensionless parameters $\tilde{\delta}_{23}^{LR}$ and $\tilde{\delta}_{32}^{LR}$ are trivially related to the previously introduced ones δ_{23}^{LR} and δ_{32}^{LR} of Eq.(8) by:

$$\delta_{23}^{LR} = \left(\frac{v_1}{m_{\text{SUSY}}} \right) \tilde{\delta}_{23}^{LR}, \quad \delta_{32}^{LR} = \left(\frac{v_1}{m_{\text{SUSY}}} \right) \tilde{\delta}_{32}^{LR}. \quad (16)$$

It is clear from Eq.(16) that δ_{23}^{LR} and δ_{32}^{LR} scale with m_{SUSY} as $\sim \frac{1}{m_{\text{SUSY}}}$. Therefore, in the forthcoming analysis of the LFV observables, whenever the decoupling behavior of these observables with large m_{SUSY} be explored we will use instead the more suited parameters $\tilde{\delta}_{23}^{LR}$ and $\tilde{\delta}_{32}^{LR}$, which can be kept fixed to a constant value while taking large m_{SUSY} values.

Concerning the size of the flavor violating trilinear couplings that are of relevance here, \mathcal{A}_{23}^l and \mathcal{A}_{32}^l , there are well-known theoretical upper bounds that arise from vacuum stability. If any of these trilinear couplings is too large, the MSSM scalar potential develops a charge and/or color breaking (CCB) minimum deeper than the Standard-Model-like (SML) local minimum or an unbounded from below (UFB) direction in the field space [25]. Then the requirement of the absence of these dangerous CCB minima or UFB directions implies specific upper bounds on the size of the non-diagonal trilinear couplings, and consequently on the size of the flavor changing deltas. For the case of interest here the upper bound from stability can be written simply as [25]:

$$|\mathcal{A}_{23}^l| \leq y_\tau \sqrt{m_{\tilde{L}_2}^2 + m_{\tilde{E}_3}^2 + m_1^2}, \quad (17)$$

and similarly for \mathcal{A}_{32}^l . Here,

$$y_\tau = \frac{gm_\tau}{\sqrt{2}M_W \cos \beta} \quad (18)$$

is the Yukawa coupling of the tau lepton, and the squared soft mass m_1^2 can be written as:

$$m_1^2 = (m_A^2 + M_W^2 + M_Z^2 \sin^2 \theta_W) \sin^2 \beta - \frac{1}{2}M_Z^2. \quad (19)$$

In our simplified scenarios for the slepton, gaugino and Higgs sectors, with just three MSSM input parameters, m_{SUSY} , $\tan \beta$, and m_A , and by considering Eqs.(15) and (16), the previous bound implies in turn the following bound on δ_{23}^{LR} , and correspondingly on $\tilde{\delta}_{23}^{LR}$ (and similar bounds for $2 \leftrightarrow 3$):

$$|\delta_{23}^{LR}| \leq \frac{m_\tau}{m_{\text{SUSY}}} \sqrt{2 + \frac{m_1^2}{m_{\text{SUSY}}^2}}, \quad |\tilde{\delta}_{23}^{LR}| \leq y_\tau \sqrt{2 + \frac{m_1^2}{m_{\text{SUSY}}^2}}. \quad (20)$$

For example, if we take $m_{\text{SUSY}} = m_A = 1$ TeV we get upper bounds for $|\tilde{\delta}_{23}^{LR}|$ of $\mathcal{O}(0.1)$ in the low $\tan \beta$ region close to 5, and of $\mathcal{O}(1)$ in the large $\tan \beta$ region close to 50. These correspond to an upper bound on $|\delta_{23}^{LR}|$ of ~ 0.0035 that is nearly independent on $\tan \beta$ and it gets weaker for larger m_{SUSY} values due to the scaling factor ($\frac{m_\tau}{m_{\text{SUSY}}}$) in Eq.(20).

However, the reliability of these bounds have been questioned in the literature because of the fact that the existence of deeper minima than the SML local minimum does not necessarily imply a problem whenever the lifetime of this false SML vacuum is sufficiently long. In this later case, other theoretical upper bounds based on metastability then apply. Indeed, by demanding that the lifetime of the whole observable universe staying at the SML vacuum be longer than the age of the universe the constraints on the flavor changing deltas get much more relaxed [26]. According to [26] the upper bounds on δ_{23}^{LR} from metastability, in contrast to the limits from stability, turn out to be independent on the Yukawa coupling, they do not decouple for asymptotically large m_{SUSY} and they are dependent on $\tan \beta$. For instance, for $\tan \beta = 3$ and $m_{\text{SUSY}} = 5$ TeV the metastability limit on δ_{23}^{LR} gets weaker than its stability bound by a factor of 40, whereas for $\tan \beta = 30$ and $m_{\text{SUSY}} = 5$ TeV it is weaker by a smaller factor of 4, leading to approximate upper bounds of $|\delta_{23}^{LR}| \leq 0.02$ and $|\delta_{23}^{LR}| \leq 0.002$ respectively. This translates into an upper bound of about $|\tilde{\delta}_{23}^{LR}| \leq 2 - 3$ for $3 \leq \tan \beta \leq 30$ and $m_{\text{SUSY}} \leq 10$ TeV. The numerical estimates of these metastability bounds are done considering each delta separately (i.e setting the other deltas to zero value) and for a specific assumption of the relevant Euclidean action providing the decay probability via tunneling of the metastable vacuum into the global minimum. Changing the input value for the Euclidean action can increase notably the maximum allowed value up to almost doubling it, leading to roughly $|\tilde{\delta}_{23}^{LR}| \leq 4 - 6$. The effects on these bounds from switching on more than one delta at the same time have not been considered yet in the literature but they could relevantly modify these bounds.

For the present work, and given the uncertainty in all these estimates of the upper bounds from stability and metastability arguments, we will consider a rather generous interval when performing the numerical estimates of branching ratios and event rates. Concretely we will choose several examples for $\tilde{\delta}_{23}^{LR}$ of very different size that will be taken within the wide interval $|\tilde{\delta}_{23}^{LR}| \leq 10$. This corresponds to $|\delta_{23}^{LR}| \leq 0.009$ for the particular values of $m_{\text{SUSY}} = 5$ TeV and $\tan \beta = 40$.

On the other hand, the values of the soft masses of the squark sector are irrelevant for LFV processes, except in the present case of LFV MSSM Higgs bosons decays where these parameters enter in the prediction of the radiatively corrected Higgs boson masses. Since we want to identify the discovered boson with the lightest MSSM Higgs boson, we will set these parameters to values which give a prediction of m_h compatible with the LHC data. Specifically, we fix them to the particular values $m_{\tilde{Q}} = m_{\tilde{U}} = m_{\tilde{D}} = A_t = A_b = 5$ TeV, which we have checked provide a value for m_h that lies within the LHC-favored range [121 GeV, 127 GeV] for all the MSSM parameter space considered here.

In summary, the input parameters of our simplified SUSY scenarios are: the mass of the pseudoscalar Higgs boson, m_A , the ratio of the two Higgs vacuum expectation values, $\tan \beta$, the generic SUSY mass scale, m_{SUSY} , and the four delta parameters, δ_{23}^{LL} , δ_{23}^{RR} , δ_{23}^{LR} and δ_{23}^{RL} (or $\tilde{\delta}_{23}^{LR}$ and $\tilde{\delta}_{23}^{RL}$ alternatively to the two latter), which we vary within the following intervals:

- $200 \text{ GeV} \leq m_A \leq 1000 \text{ GeV}$,
- $1 \leq \tan \beta \leq 60$,
- $0.5 \text{ TeV} \leq m_{\text{SUSY}} \leq 10 \text{ TeV}$,
- $-1 \leq \delta_{23}^{LL}, \delta_{23}^{RR} \leq 1$,
- $-10 \leq \tilde{\delta}_{23}^{LR}, \tilde{\delta}_{23}^{RL} \leq 10$,
(or, equivalently, $|\delta_{23}^{LR}|, |\delta_{23}^{RL}| \leq 0.009$ for $m_{\text{SUSY}} = 5$ TeV and $\tan \beta = 40$).

3 Results for the branching ratios of the LFV decays

In this section we study the behavior of the radiative corrections from SUSY loops to the LFV neutral Higgs bosons decays in the heavy SUSY particle mass limit and compare them with the case of LFV radiative lepton decays. For the forthcoming estimates of the LFV Higgs decay rates, we use the complete one-loop formulas and the full set of diagrams contributing to the $\Gamma(\phi \rightarrow \bar{l}_i l_j)$ and $\Gamma(\phi \rightarrow l_i \bar{l}_j)$ partial decay widths, with $i \neq j$, within the MSSM, which are written in terms of the mass eigenvalues for all the involved MSSM sparticles, including the physical slepton and sneutrino masses, $m_{\tilde{l}_i}$ ($i = 1, \dots, 6$) and $m_{\tilde{\nu}_i}$ ($i = 1, 2, 3$), and the rotation matrices $R^{\tilde{l}}$ and $R^{\tilde{\nu}}$ of Eqs. (10) and (11). We take these general one-loop formulas from [9] and emphasize that they are valid for the general slepton mixing case considered here, with all the mixing effects from the δ_{ij}^{AB} 's being transmitted to the LFV Higgs decay rates via the physical slepton and sneutrino masses and their corresponding rotations. The off-diagonal trilinear couplings in Eq.(6) also enter into this computation of the LFV Higgs decay rates. For a more detailed discussion about these analytical results we refer the reader to [9]. It should be also noted that, since we are assuming real δ_{ij}^{AB} 's, the predictions for $\text{BR}(\phi \rightarrow l_i \bar{l}_j)$ and the CP-conjugate $\text{BR}(\phi \rightarrow \bar{l}_i l_j)$ are the same. Thus, we will perform our estimates for just one of them and will denote this rate generically by $\text{BR}(\phi \rightarrow l_i l_j)$. Obviously, in the case that these two channels cannot be differentiated experimentally one should then add the two contributions to the total final number of events. However, for the present computation we do not sum them and report instead the results for $\phi \rightarrow l_i l_j$, meaning that they are valid for any of the two cases.

As said above, we focus only on $h \rightarrow \tau\mu$, $H \rightarrow \tau\mu$ and $A \rightarrow \tau\mu$ decay channels and consider the constraints imposed over the parameter space by the current upper bound on the related LFV radiative decay $\tau \rightarrow \mu\gamma$ [23]. The SUSY mass spectra are computed numerically with the code **SPheno** [27]. The slepton and sneutrino spectra are computed from an additional subroutine that we have implemented into **SPheno** in order to include our parametrization of slepton mixing given by the δ_{ij}^{AB} 's. The LFV decay rates are computed with our private FORTRAN code in which we have implemented the complete one-loop formulas for the LFV partial Higgs decay widths of [9] and the complete one-loop formulas for the LFV radiative τ decay widths which we take from [11]. Note that these latter formulas for the $\tau \rightarrow \mu\gamma$ decays are also written in terms of the physical sparticle eigenvalues and eigenstates and do not neglect any of the lepton masses. The mass spectrum of the MSSM Higgs sector, with two-loop corrections included, and their corresponding total widths are calculated by means of the code **FeynHiggs** [28].

Next we present the numerical results for the branching ratios of the LFV decays. We show in Figure 1 the behavior of the branching ratios for the two types of LFV decays, $\text{BR}(\phi \rightarrow \tau\mu)$ and $\text{BR}(\tau \rightarrow \mu\gamma)$, as functions of m_{SUSY} , and we consider two different values of $\tan\beta$, namely, $\tan\beta = 5$ (left panels) and $\tan\beta = 40$ (right panels). In each case we set one single delta to be non vanishing with the particular values: $\delta_{23}^{LL} = 0.5$ (upper panels), $\delta_{23}^{RR} = 0.5$ (middle panels) and $\delta_{23}^{LR} = 0.5$ (lower panels). All the other flavor changing deltas are set to zero. We find identical results for $\tilde{\delta}_{23}^{RL} = 0.5$ as for $\tilde{\delta}_{23}^{LR} = 0.5$ and, for brevity, we have omitted the plots for $\tilde{\delta}_{23}^{RL}$ in Figure 1.

On the upper panels of Figure 1, when the responsible for the flavor mixing between the second and the third generations is δ_{23}^{LL} , the branching ratios of the LFV Higgs decays show a clear non-decoupling behavior with m_{SUSY} , which remain constant from $m_{\text{SUSY}} \simeq 1$ TeV to $m_{\text{SUSY}} = 10$ TeV, with values of $\text{BR}(h \rightarrow \tau\mu) \simeq 5 \times 10^{-11}$ and $\text{BR}(H, A \rightarrow \tau\mu) \simeq 8 \times 10^{-9}$ for $\tan\beta = 5$, and $\text{BR}(h \rightarrow \tau\mu) \simeq 3 \times 10^{-9}$ and $\text{BR}(H, A \rightarrow \tau\mu) \simeq 3 \times 10^{-6}$ for $\tan\beta = 40$. Another important feature that should be noted is the fast growing with $\tan\beta$ of these decays which increase the H and A LFV decay rates almost three orders of magnitude from $\tan\beta = 5$ to $\tan\beta = 40$. Furthermore, we have numerically checked that for large values of $\tan\beta \geq 10$ the partial decay widths $\Gamma(H, A \rightarrow \tau\mu)$ go approximately as $\sim (\tan\beta)^4$ [9], whereas $\Gamma(h \rightarrow \tau\mu)$ goes as $\sim (\tan\beta)^2$. This implies that the corresponding branching ratios go all at large $\tan\beta \geq 10$ as $\text{BR}(h, H, A \rightarrow \tau\mu) \sim (\tan\beta)^2$ in this LL case, since the total widths go as $\Gamma_{\text{tot}}(H, A) \sim (\tan\beta)^2$ and $\Gamma_{\text{tot}}(h)$ is approximately constant with $\tan\beta$. This behavior of the BRs with $\tan\beta$ is confirmed numerically in our forthcoming Figure 2. In contrast, the branching ratio of the $\tau \rightarrow \mu\gamma$ decay presents a decoupling behavior with m_{SUSY} , decreasing as $\sim 1/m_{\text{SUSY}}^4$, and it is reduced around five orders of magnitude from $m_{\text{SUSY}} = 500$ GeV to $m_{\text{SUSY}} = 10$ TeV. In all these figures we have also included, for comparison, the experimental upper bound for the $\tau \rightarrow \mu\gamma$ channel, whose present value is $\text{BR}(\tau \rightarrow \mu\gamma) < 4.4 \times 10^{-8}$ [23]. Thus, each m_{SUSY} point which leads to a prediction of $\text{BR}(\tau \rightarrow \mu\gamma)$ above this line is excluded by data. Therefore, only values of $m_{\text{SUSY}} \gtrsim 2$ TeV for $\tan\beta = 5$ and $m_{\text{SUSY}} \gtrsim 5$ TeV for $\tan\beta = 40$, and their corresponding predictions for the LFV rates, are allowed for $\delta_{23}^{LL} = 0.5$.

On the middle panels of Figure 1 we have plotted the LFV Higgs and radiative decay rates as functions of m_{SUSY} , considering δ_{23}^{RR} as the responsible for $\tau - \mu$ mixing. A similar non-decoupling behavior to the δ_{23}^{LL} case can be observed for δ_{23}^{RR} , whose branching ratios stay again constant as m_{SUSY} grows. However, the numerical contribution of δ_{23}^{RR} to the LFV processes is much less important than that of δ_{23}^{LL} , and all the RR rates are in comparison around two orders of magnitude smaller than the LL rates. In the RR case, another important feature is that all the predictions found of $\text{BR}(\tau \rightarrow \mu\gamma)$ for $5 \leq \tan\beta \leq 40$ and m_{SUSY} values above 500 GeV are allowed by the present $\text{BR}(\tau \rightarrow \mu\gamma)$ experimental upper bound.

The predictions of $\text{BR}(h \rightarrow \tau\mu)$, $\text{BR}(H \rightarrow \tau\mu)$, $\text{BR}(A \rightarrow \tau\mu)$ and $\text{BR}(\tau \rightarrow \mu\gamma)$ as functions of m_{SUSY} , for the case $\tilde{\delta}_{23}^{LR} = 0.5$, are shown on the lower panels of Figure 1. We see clearly

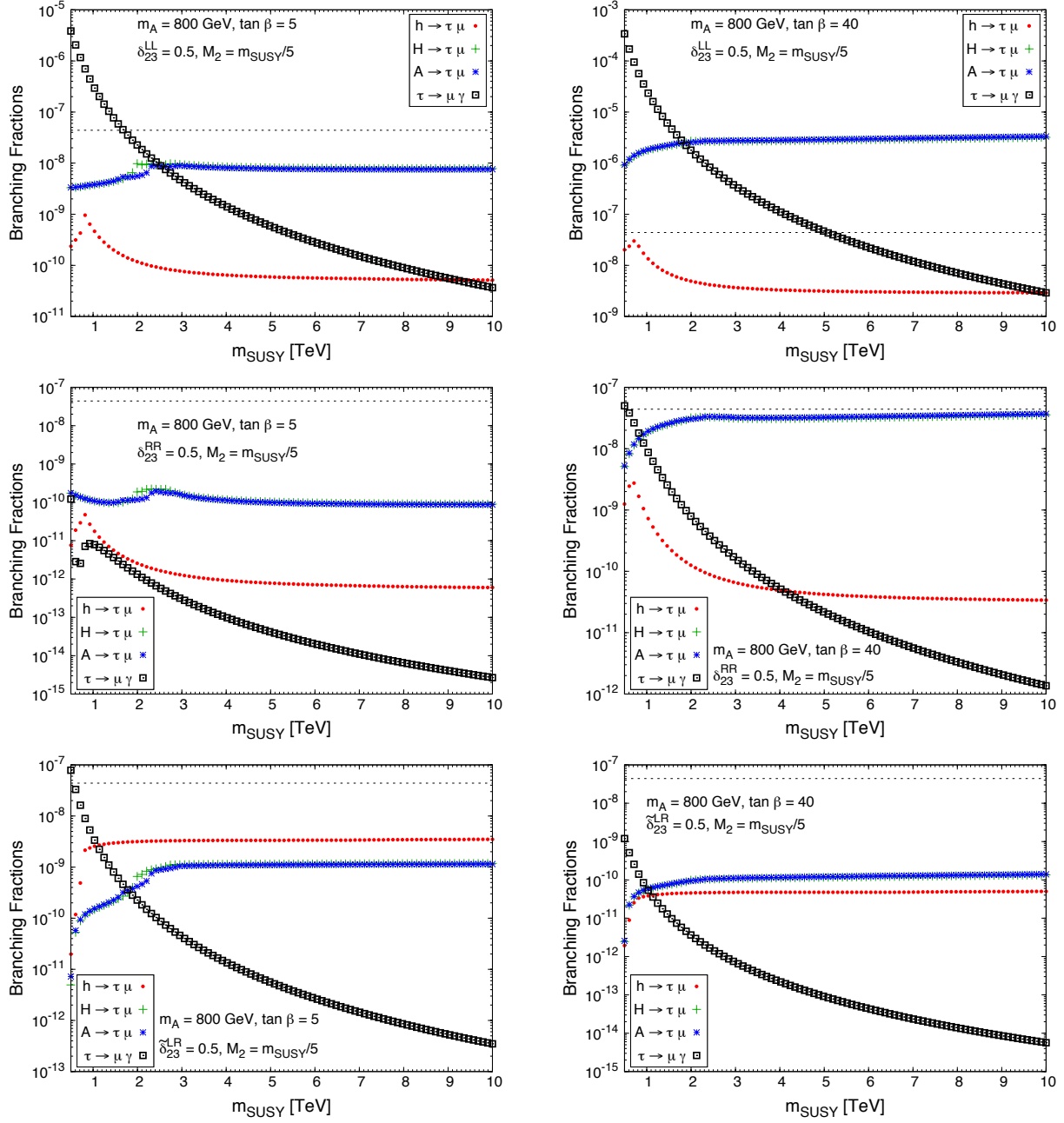


Figure 1: Large m_{SUSY} behaviour of the LFV decay rates: $\text{BR}(h \rightarrow \tau\mu)$, $\text{BR}(H \rightarrow \tau\mu)$, $\text{BR}(A \rightarrow \tau\mu)$ and $\text{BR}(\tau \rightarrow \mu\gamma)$ as functions of m_{SUSY} for $\tan\beta = 5$ (left panels) and $\tan\beta = 40$ (right panels) with $\delta_{23}^{LL} = 0.5$ (upper panels), $\delta_{23}^{RR} = 0.5$ (middle panels) and $\tilde{\delta}_{23}^{LR} = 0.5$ (lower panels). The results for $\tilde{\delta}_{23}^{RL} = 0.5$ (not shown) are identical to those of $\tilde{\delta}_{23}^{LR} = 0.5$. In each case, the other flavor changing deltas are set to zero. In all panels, $m_A = 800$ GeV and the other MSSM parameters are set to the values reported in the text, with $M_2 = \frac{1}{5}m_{\text{SUSY}}$. The horizontal dashed line denotes the current experimental upper bound for $\tau \rightarrow \mu\gamma$ channel, $\text{BR}(\tau \rightarrow \mu\gamma) < 4.4 \times 10^{-8}$ [23].

again a non-decoupling behavior with m_{SUSY} , since the branching ratios of the Higgs decays tend

to a constant value as m_{SUSY} grows, in contrast to the $\text{BR}(\tau \rightarrow \mu\gamma)$ rates that display again a decoupling behavior and decrease with m_{SUSY} . For this particular choice of $\tilde{\delta}_{23}^{LR} = 0.5$ we also see that the predicted branching ratios for the LFV h decays at low $\tan\beta = 5$ are larger than in the previous LL and RR cases, whereas the branching ratios for the LFV H and A decays are larger than those of the RR case but smaller than the LL ones. The lower right panel shows that for $\tan\beta = 40$ the branching ratios of the three Higgs bosons, h , H and A , are comparatively smaller than for $\tan\beta = 5$. This decreasing with $\tan\beta$ of the LFV decay rates for the LR case with fixed value of $\tilde{\delta}_{23}^{LR}$ is confirmed in our forthcoming Figure 2. In consequence, the largest LFV Higgs decay rates that will be obtained in the LR (and RL) case will be for low $\tan\beta$ values and this will be taken into account in our next studies in order to maximize the event rates from these decays at the LHC.

To sum up the main results of Figure 1, the most relevant δ_{23}^{AB} parameter at low $\tan\beta$ values for the lightest Higgs boson h is $\tilde{\delta}_{23}^{LR}$ (and $\tilde{\delta}_{23}^{RL}$), which gives rise to larger LFV Higgs decay rates than δ_{23}^{LL} and δ_{23}^{RR} , whereas for the H and A Higgs bosons the most relevant parameter is δ_{23}^{LL} . At large $\tan\beta$ values, the most relevant parameter for all the three Higgs bosons is δ_{23}^{LL} . All these branching ratios, as we will see later, can be further enhanced by considering two non-vanishing deltas at the same time, by exploring with larger size of these deltas, and also by considering different signs for the various deltas. Overall, the main conclusion from this Figure 1 is that if one wants to obtain sizeable and allowed by data branching ratios, one needs large values of m_{SUSY} , which plays a double role: on one hand, it keeps constant values of the LFV Higgs decay rates (due to the non-decoupling behavior of these decays with m_{SUSY}) and, on the other hand, it brings down $\tau \rightarrow \mu\gamma$ below its experimental upper bound (because of the decoupling effect of LFV radiative decays with m_{SUSY}).

As we have said above, we show in Figure 2 the behavior of LFV branching ratios as functions of $\tan\beta$ for $\delta_{23}^{LL} = 0.5$ (upper left panel), $\delta_{23}^{RR} = 0.5$ (upper right panel), $\tilde{\delta}_{23}^{LR} = 0.5$ (lower left panel) and $\tilde{\delta}_{23}^{RL} = 0.5$ (lower right panel) with $m_A = 1000$ GeV, $m_{\text{SUSY}} = 5$ TeV and $M_2 = m_{\text{SUSY}}/5$. All the LFV rates have a very similar behavior with $\tan\beta$ for both LL and RR mixing cases and grow as $\sim (\tan\beta)^2$ for large values of $\tan\beta \gtrsim 10$, as indicated in the previous paragraphs. In contrast, the LFV rates present a decreasing behavior with $\tan\beta$ in the LR and RL cases, which are identical. $\text{BR}(\tau \rightarrow \mu\gamma)$ and $\text{BR}(h \rightarrow \tau\mu)$ go approximately as $\sim (\tan\beta)^{-2}$ while $\text{BR}(H \rightarrow \tau\mu)$ and $\text{BR}(A \rightarrow \tau\mu)$ grow around two orders of magnitude from $\tan\beta = 1$ to $\tan\beta = 5$, and from this value decrease in the same way as $\tau \rightarrow \mu\gamma$ and $h \rightarrow \tau\mu$. Therefore, within the large $\tan\beta$ regime ($\tan\beta \gtrsim 10$), in the LL and RR mixing cases the LFV rates grow as $\sim (\tan\beta)^2$ whilst in the LR and RL ones these rates present the opposite behavior and decrease as $\sim (\tan\beta)^{-2}$.

Now, we are interested in investigating if other choices of M_2 alter these previous results. For this purpose, we have plotted in Figure 3 the predictions of $\text{BR}(h \rightarrow \tau\mu)$ (dots in upper panels), $\text{BR}(A \rightarrow \tau\mu)$ (dots in lower panels) and $\text{BR}(\tau \rightarrow \mu\gamma)$ (crosses in all panels) as functions of m_{SUSY} for different values of a (see Eq. (13)), $a = 1$ (in red), $a = \frac{1}{3}$ (in green) and $a = \frac{1}{5}$ (in blue), with $\delta_{23}^{LL} = 0.5$ (left panels) and $\tilde{\delta}_{23}^{LR} = \tilde{\delta}_{23}^{RL} = 0.5$ (right panels). The results for the $H \rightarrow \tau\mu$ channel are nearly identical to those of $A \rightarrow \tau\mu$ and not shown here for shortness. In the case of LL mixing, all the LFV Higgs rates, which present the same behavior with a , increase around a factor of 7 from $a = \frac{1}{5}$ to $a = 1$, while the $\tau \rightarrow \mu\gamma$ rates present the opposite behavior with a , decreasing in a factor about 40 for the same values of a . Therefore, if δ_{23}^{LL} is the responsible for the slepton mixing, and for the explored interval $1/5 \leq a \leq 1$, the larger M_2 is (and consequently M_1 and μ), the larger the LFV Higgs branching ratios are and the lower $\text{BR}(\tau \rightarrow \mu\gamma)$ is. In the LR -mixing case we see that again $\text{BR}(h, H, A \rightarrow \tau\mu)$ rise as a grows and the enhancement is by a large factor of about 15 by changing $a = \frac{1}{5}$ to $a = 1$. In contrast to the LL case, $\text{BR}(\tau \rightarrow \mu\gamma)$ also increases with a for LR mixing, although softer than the LFV Higgs rates. In summary, we learn from Figure 3

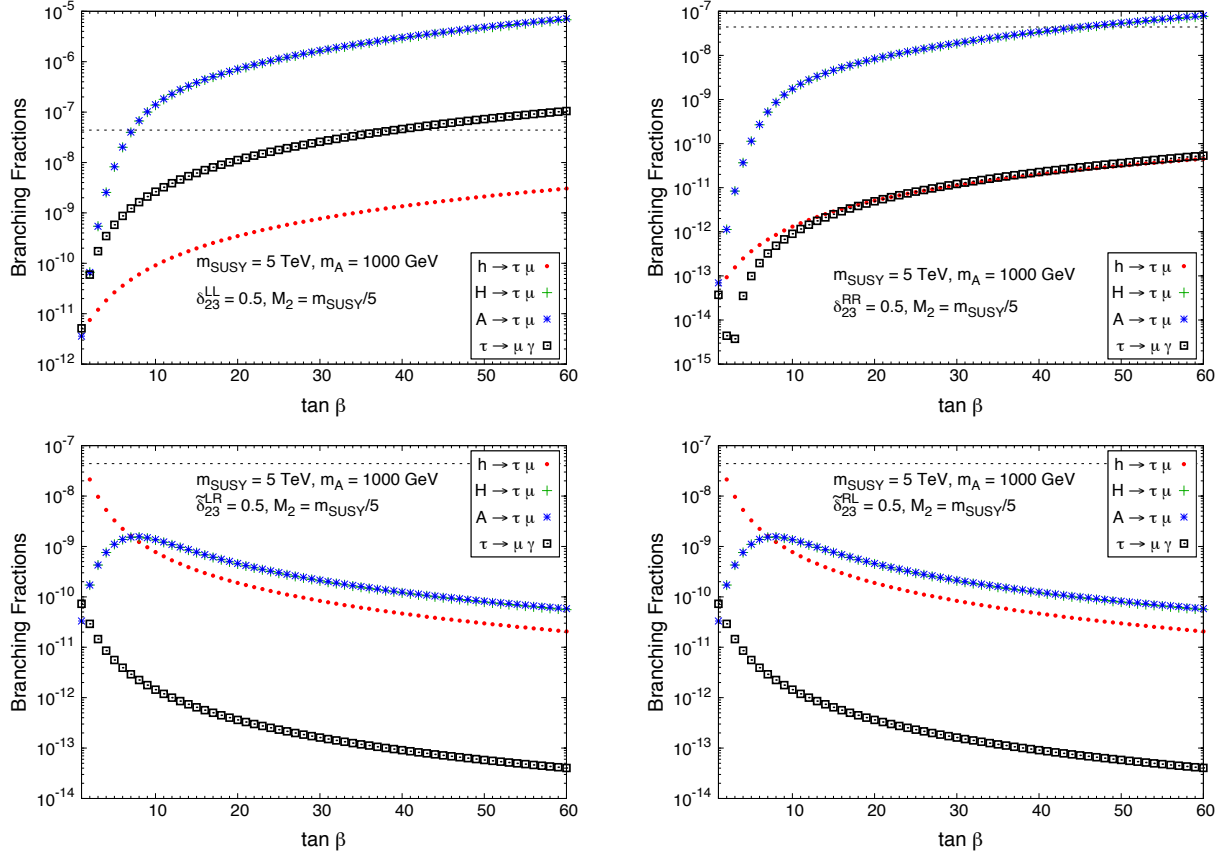


Figure 2: $\text{BR}(h \rightarrow \tau\mu)$, $\text{BR}(H \rightarrow \tau\mu)$, $\text{BR}(A \rightarrow \tau\mu)$ and $\text{BR}(\tau \rightarrow \mu\gamma)$ as functions of $\tan\beta$ for $\delta_{23}^{LL} = 0.5$ (upper left panel), $\delta_{23}^{RR} = 0.5$ (upper right panel), $\delta_{23}^{LR} = 0.5$ (lower left panel) and $\delta_{23}^{RL} = 0.5$ (lower right panel). In each case, the other flavor changing deltas are set to zero. In all panels, $m_A = 1000$ GeV, $m_{\text{SUSY}} = 5$ TeV and the other MSSM parameters are set to the values reported in the text, with $M_2 = m_{\text{SUSY}}/5$. The horizontal dashed line denotes the current experimental upper bound for $\tau \rightarrow \mu\gamma$ channel, $\text{BR}(\tau \rightarrow \mu\gamma) < 4.4 \times 10^{-8}$ [23].

that the best choice, for a fixed delta parameter, in order to obtain the largest LFV Higgs rates is $M_2 = m_{\text{SUSY}}$. However, we must be very careful, because it is possible that these large rates are excluded by the $\tau \rightarrow \mu\gamma$ upper bound, depending basically on the specific values of δ_{23}^{LL} , δ_{23}^{LR} and $\tan\beta$.

In order to look into the largest values of δ_{23}^{AB} allowed by data for the choice $M_2 = m_{\text{SUSY}}$, we show in Figure 4 the results of the branching fractions for the LFV Higgs decays into $\tau\mu$ and the related LFV radiative decay $\tau \rightarrow \mu\gamma$ as functions of the four deltas considered along this work. We have fixed in these plots $\tan\beta = 40$. For completeness, we have also presented here the results for δ_{23}^{RR} , which are irrelevant for the present work since all the branching ratios obtained are extremely small to be detectable at the LHC, and the δ_{23}^{RL} results, which are identical to the δ_{23}^{LR} ones. The plots in Figure 4 show the expected growing of the LFV rates with the $|\delta_{23}^{AB}|$'s, and all of them are clearly symmetric $\delta_{23}^{AB} \rightarrow -\delta_{23}^{AB}$. On the upper left panel we have the results for the LL case and it is clear that all the values of δ_{23}^{LL} , from -1 to 1 , are allowed by data, due to the large suppression that $\tau \rightarrow \mu\gamma$ suffers for $m_{\text{SUSY}} = 5$ TeV. The predictions for $H \rightarrow \tau\mu$ (green crosses)

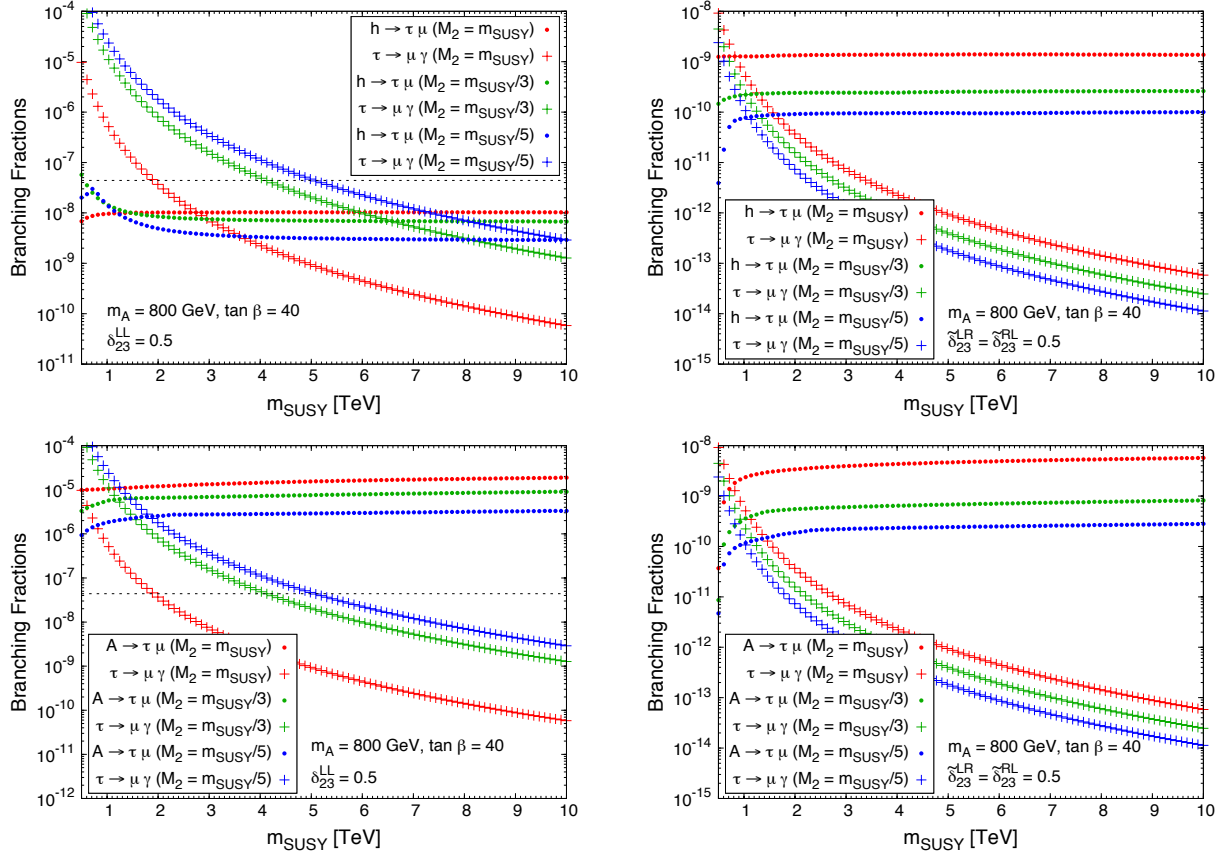


Figure 3: Sensitivity to M_2 : LFV Higgs decay rates (dots) and $\text{BR}(\tau \rightarrow \mu\gamma)$ (crosses) as functions of m_{SUSY} with $\delta_{23}^{LL} = 0.5$ (left panels) and $\tilde{\delta}_{23}^{LR} = \tilde{\delta}_{23}^{RL} = 0.5$ (right panels) for different choices of M_2 : $M_2 = m_{\text{SUSY}}$ (in red), $M_2 = \frac{1}{3}m_{\text{SUSY}}$ (in green) and $M_2 = \frac{1}{5}m_{\text{SUSY}}$ (in blue). The results for H (not shown) are nearly identical to those of A . In each case, the other flavor changing deltas are set to zero. In all panels, $m_A = 800$ GeV, $\tan \beta = 40$ and the other MSSM parameters are set to the values reported in the text. The horizontal dashed line denotes the current experimental upper bound for $\tau \rightarrow \mu\gamma$ channel, $\text{BR}(\tau \rightarrow \mu\gamma) < 4.4 \times 10^{-8}$ [23].

are indistinguishable from $A \rightarrow \tau\mu$ ones (blue asterisks), which are superimposed in these plots. One can reach values of $\text{BR}(h \rightarrow \tau\mu) \simeq 10^{-7}$ and $\text{BR}(H, A \rightarrow \tau\mu) \simeq 2 \times 10^{-4}$ at the most for $\delta_{23}^{LL} = \pm 1$. The predictions for the LFV rates as functions of δ_{23}^{LR} are presented on the lower left panel of Figure 4. In this case, all the values of $|\delta_{23}^{LR}|$ are allowed by the $\tau \rightarrow \mu\gamma$ upper bound and the largest value of $|\delta_{23}^{LR}| \simeq 0.009$ (which corresponds to $\tilde{\delta}_{23}^{LR} \simeq 10$) gives rise to a branching fraction of 3×10^{-7} for the $h \rightarrow \tau\mu$ channel, while $\text{BR}(H, A \rightarrow \tau\mu)$ reach values of 1×10^{-6} . The low rates in the $h \rightarrow \tau\mu$ channel for this LR -mixing case can be notably increased, as we have said previously, by assuming a lower $\tan \beta$ value closer to the low $\tan \beta$ region with $\tan \beta \lesssim 5$.

Finally, we have studied the possibility of switching on several deltas simultaneously. Specifically, we have fixed $\delta_{23}^{LL} = 0.9$ and considered different choices of $\tilde{\delta}_{23}^{LR} = \tilde{\delta}_{23}^{RL}$ with either negative values: $(-0.7, -2$ and $-10)$, or positive values $(+0.7, +2$ and $+10)$. The results are depicted in Figure 5 for the case of low $\tan \beta = 5$ that is the most interesting one since the LL and LR (and RL) contributions are of similar size and their interferences can be relevant for some regions of the

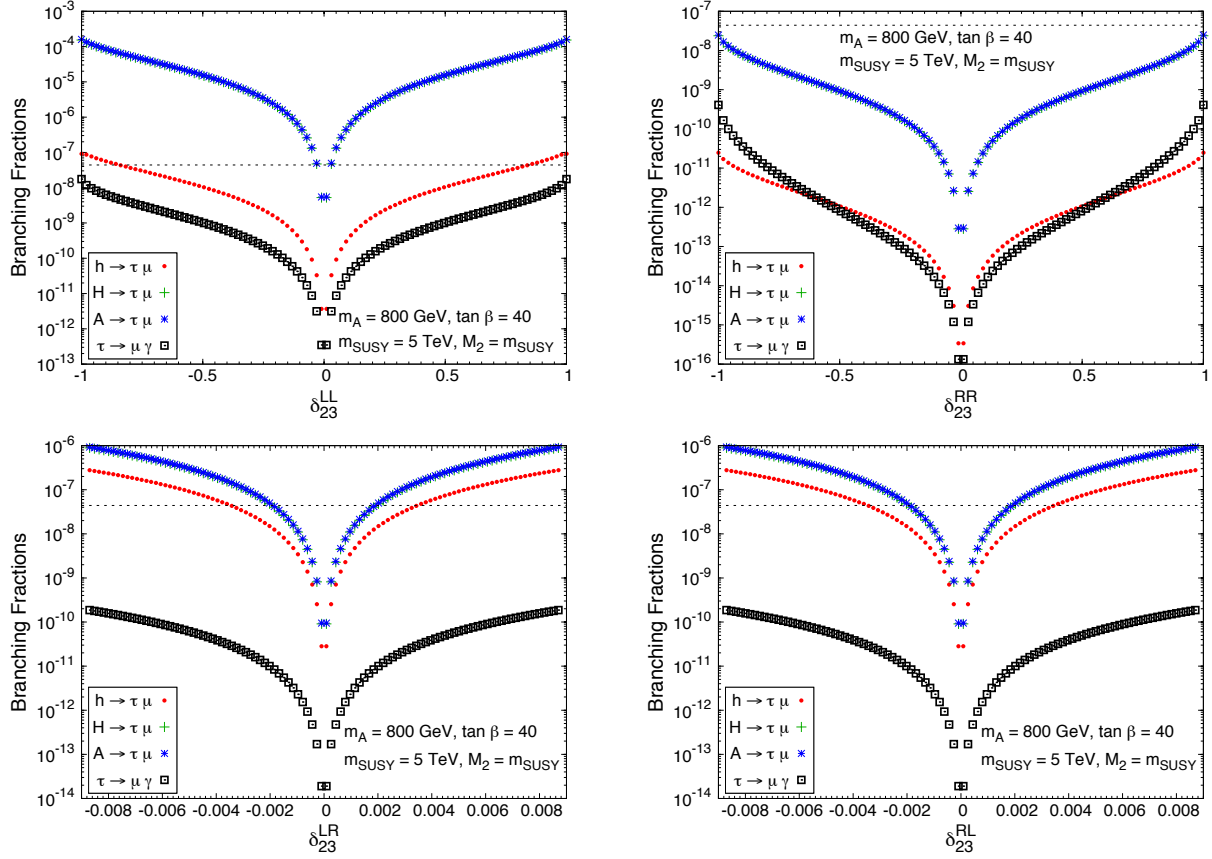


Figure 4: $\text{BR}(h \rightarrow \tau\mu)$, $\text{BR}(H \rightarrow \tau\mu)$, $\text{BR}(A \rightarrow \tau\mu)$ and $\text{BR}(\tau \rightarrow \mu\gamma)$ as functions of δ_{23}^{LL} (upper left panel), δ_{23}^{RR} (upper right panel), δ_{23}^{LR} (lower left panel) and δ_{23}^{RL} (lower right panel). In each case, the other flavor changing deltas are set to zero. In all panels, $m_A = 800$ GeV, $\tan\beta = 40$, $m_{\text{SUSY}} = 5$ TeV and the other MSSM parameters are set to the values reported in the text, with $M_2 = m_{\text{SUSY}}$. The horizontal dashed line denotes the current experimental upper bound for $\tau \rightarrow \mu\gamma$ channel, $\text{BR}(\tau \rightarrow \mu\gamma) < 4.4 \times 10^{-8}$ [23].

parameter space. As expected, the four LFV decay rates increase as $|\tilde{\delta}_{23}^{LR}| = |\tilde{\delta}_{23}^{RL}|$ grows, and they are slightly higher than for single LL or LR mixings. The most important conclusion in this case is that we are able to obtain large branching ratios for all the three LFV Higgs decays, reaching values close to 10^{-4} for h and about 3×10^{-5} for A and H , if $\tilde{\delta}_{23}^{LR} = \tilde{\delta}_{23}^{RL} = \pm 10$. By comparing the results for negative versus positive LR mixings, we also learn from this figure that there are not relevant differences. The LFV Higgs decay rates for negative mixings are slightly higher than the corresponding rates for positive mixings, and this difference is more visible in the A and H LFV decays than in the h LFV decay. It should also be noted that the rates for $\tau \rightarrow \mu\gamma$ decays go the other way around, namely, they are slightly larger for positive LR mixings than for negative LR mixings, indicating that the interference between the LL and LR contributions must be of opposite sign in the LFV Higgs decays versus the $\tau \rightarrow \mu\gamma$ decays.

To close this section, we can conclude from Figures 1, 2, 3, 4 and 5 that, for the explored intervals of the parameter space, the largest LFV Higgs rates that are allowed by the $\tau \rightarrow \mu\gamma$ upper bound are obtained for the following values of the model parameters: large $m_{\text{SUSY}} \gtrsim 5$ TeV, M_2 close to

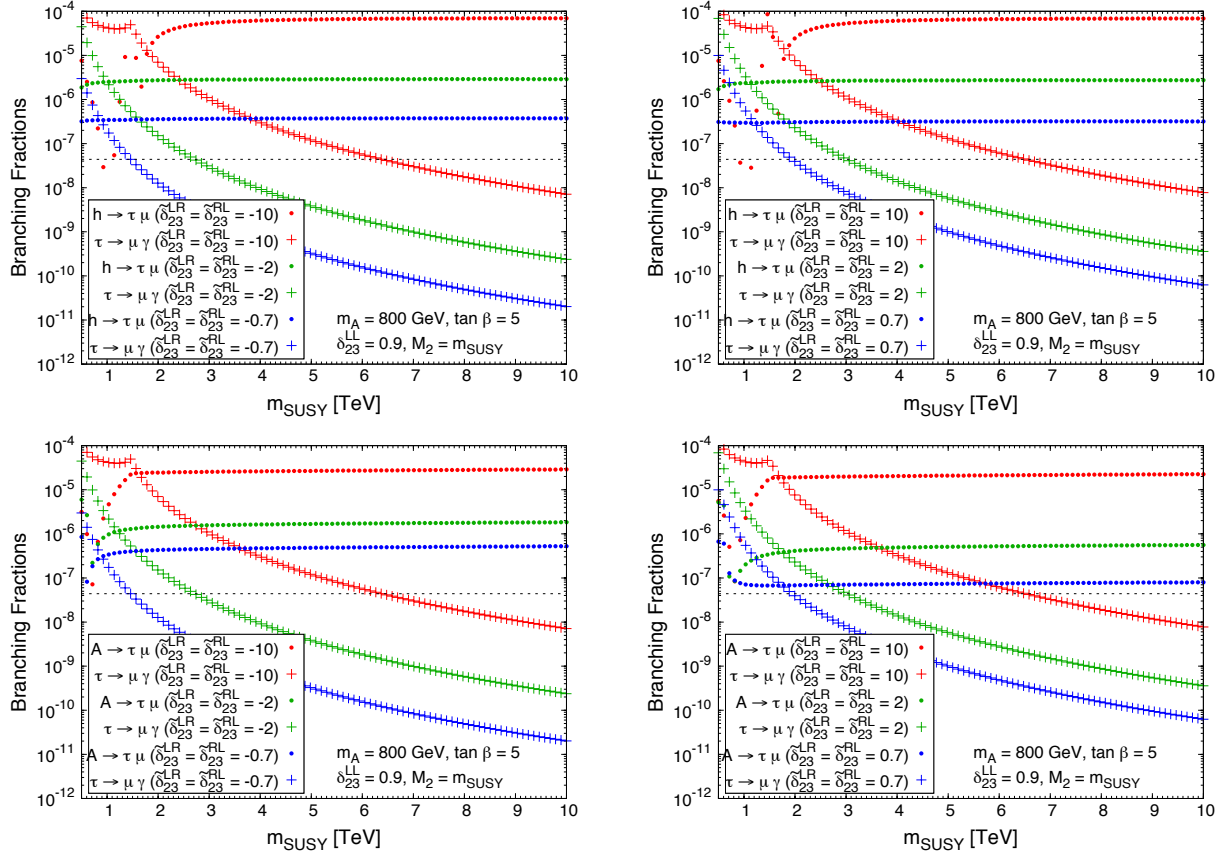


Figure 5: Sensitivity to double LL and LR mixing deltas: LFV Higgs decay rates (dots) and $\text{BR}(\tau \rightarrow \mu\gamma)$ (crosses) as functions of m_{SUSY} with $\delta_{23}^{LL} = 0.9$ for different choices of negative LR mixing (left panels), $\tilde{\delta}_{23}^{LR} = \tilde{\delta}_{23}^{RL}$: -0.7 (in blue), -2 (in green) and -10 (in red), and of positive LR mixing (right panels), $\tilde{\delta}_{23}^{LR} = \tilde{\delta}_{23}^{RL}$: $+0.7$ (in blue), $+2$ (in green) and $+10$ (in red). The results for H (not shown) are nearly identical to those of A . In each case, the other flavor changing deltas are set to zero. In both panels, $m_A = 800$ GeV, $\tan\beta = 5$, $M_2 = m_{\text{SUSY}}$ and the other MSSM parameters are set to the values reported in the text. The horizontal dashed line denotes the current experimental upper bound for $\tau \rightarrow \mu\gamma$ channel, $\text{BR}(\tau \rightarrow \mu\gamma) < 4.4 \times 10^{-8}$ [23].

m_{SUSY} and $|\delta_{23}^{LL}|$ and $|\tilde{\delta}_{23}^{LR}|$ (and/or $|\tilde{\delta}_{23}^{RL}|$) close to their maximum explored values of 1 and 10, respectively. According to these previous findings, in the forthcoming computation of cross sections and event rates at the LHC, whenever we have to fix them, we will set the following particular reference model parameters: $m_{\text{SUSY}} = 5$ TeV, $M_2 = m_{\text{SUSY}}$, $\delta_{23}^{LL} = 0.9$ and $\tilde{\delta}_{23}^{LR} = \tilde{\delta}_{23}^{RL} = \pm 5$, which are approximately the largest allowed values by the metastability bounds. The corresponding predictions for other choices of δ_{23}^{LL} , $\tilde{\delta}_{23}^{LR}$, $\tilde{\delta}_{23}^{RL}$, M_2 , m_{SUSY} and $\tan\beta$ can be easily derived from these first five figures.

4 Results for the LFV event rates at the LHC

In this section we present the results of the LFV event rates at the LHC which are mediated by the production of neutral MSSM Higgs bosons and their subsequent LFV decays into $\tau\mu$. The

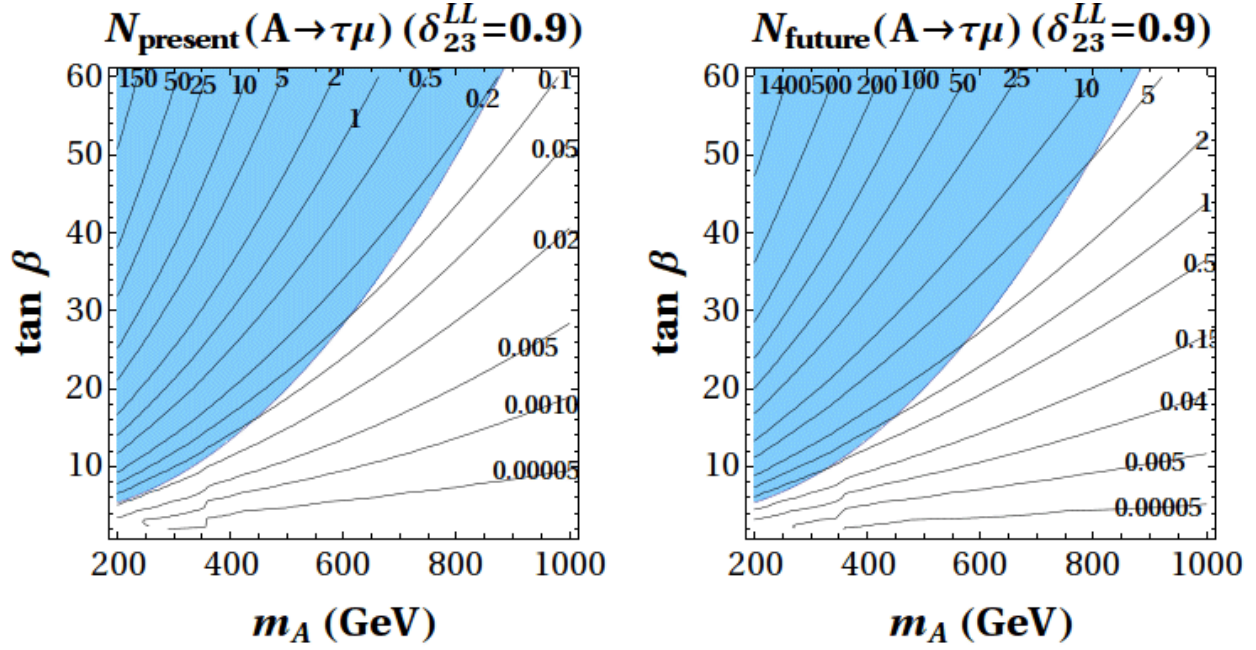


Figure 6: Number of expected LFV events in the $(m_A, \tan \beta)$ plane from $A \rightarrow \tau \mu$ for $\delta_{23}^{LL} = 0.9$ and $m_{\text{SUSY}} = 5$ TeV. Left panel: present phase of the LHC with $\sqrt{s} = 8$ TeV and $\mathcal{L} = 25 \text{ fb}^{-1}$. Right panel: future phase of the LHC with $\sqrt{s} = 14$ TeV and $\mathcal{L} = 100 \text{ fb}^{-1}$. In both panels the other MSSM parameters are set to the values reported in the text, with $M_2 = m_{\text{SUSY}}$. The shaded blue areas are excluded by CMS searches [29]. The results for H (not shown) are nearly equal to these ones for A .

production cross sections of the neutral Higgs bosons are calculated here by means of the code **FeynHiggs** [28]. For low values of $\tan \beta$, the production cross sections of the three neutral MSSM Higgs bosons are dominated by gluon fusion. By contrast, for moderate and large values of $\tan \beta$ ($\gtrsim 10$), the production cross sections of H and A Higgs bosons via bottom-antibottom quark annihilation become the dominant ones, while the h production cross section is still dominated by gluon fusion. In the following, we consider center-of-mass energies at the LHC of $\sqrt{s} = 8$ TeV, with a total integrated luminosity of $\mathcal{L} = 25 \text{ fb}^{-1}$, and $\sqrt{s} = 14$ TeV, with $\mathcal{L} = 100 \text{ fb}^{-1}$, and focus on the two cases with the largest LFV Higgs decay rates, with either LL or LR or both slepton $\tau - \mu$ mixings. Although we do not expect any competitive background to these singular LFV signals at the LHC, a more realistic and devoted study of the potential backgrounds should be done, but this is beyond the scope of this paper.

Once we have set up the most relevant parameters for the present study of LFV at the LHC, which are the two flavor mixing deltas δ_{23}^{LL} and δ_{23}^{LR} (and correspondingly δ_{23}^{RL}), m_{SUSY} and $\tan \beta$, we will present next the results for the final rates at the LHC, both in the present and future phases, in the most convenient way for comparison with future experimental analysis, namely, in the $(m_A, \tan \beta)$ plane. Since the results for the $H \rightarrow \tau \mu$ event rates turn out to be nearly equal to those of the $A \rightarrow \tau \mu$ ones, we will not exhibit them here for shortness. Thus we will focus on the LFV rates of h and A decays. In the following plots we have also specified the areas of the $(m_A, \tan \beta)$ plane (blue areas) that are excluded by the recent CMS searches for MSSM neutral Higgs bosons decaying to $\tau \bar{\tau}$ pairs in the so-called m_h^{max} scenario [29]. All the predictions shown

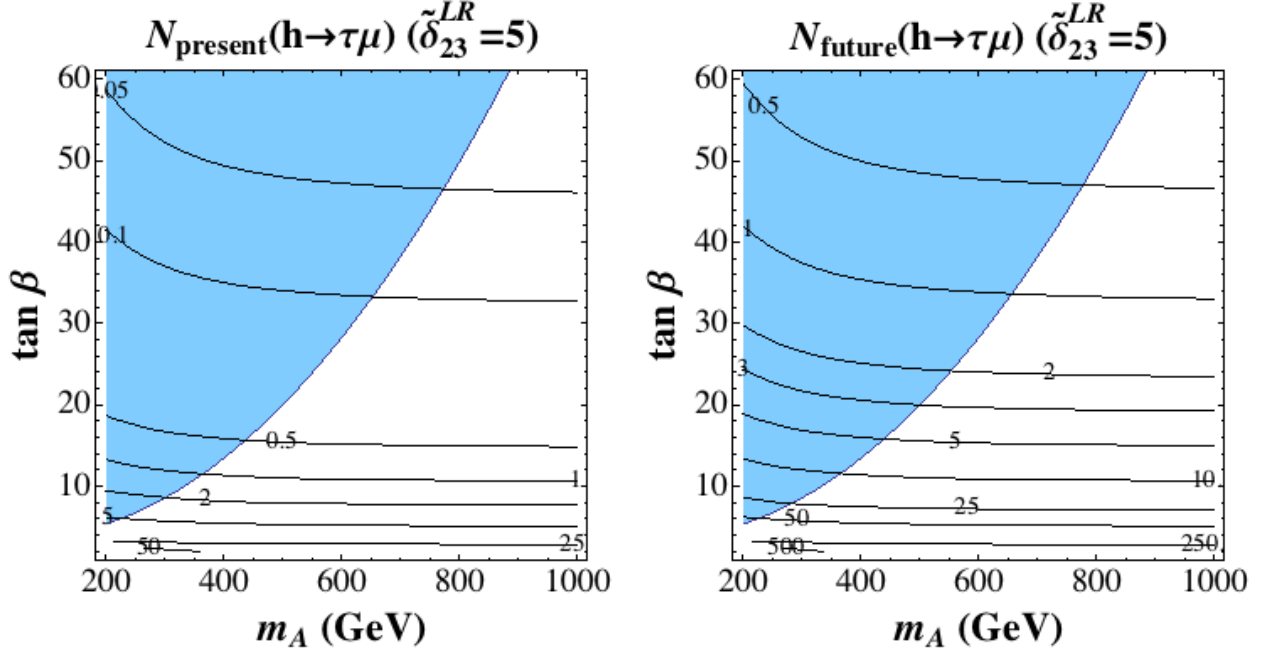


Figure 7: Number of expected LFV events in the $(m_A, \tan \beta)$ plane from $h \rightarrow \tau \mu$ for $\tilde{\delta}_{23}^{LR} = \tilde{\delta}_{23}^{RL} = 5$ and $m_{\text{SUSY}} = 5$ TeV. Left panel: present phase of the LHC with $\sqrt{s} = 8$ TeV and $\mathcal{L} = 25 \text{ fb}^{-1}$. Right panel: future phase of the LHC with $\sqrt{s} = 14$ TeV and $\mathcal{L} = 100 \text{ fb}^{-1}$. In both panels the other MSSM parameters are set to the values reported in the text, with $M_2 = m_{\text{SUSY}}$. The shaded blue areas are excluded by CMS searches [29].

next are allowed by the present $\tau \rightarrow \mu \gamma$ upper bound.

We start this analysis with the LL case and plot in Figure 6 the number of events expected in the $(m_A, \tan \beta)$ plane for the $A \rightarrow \tau \mu$ channel with $\delta_{23}^{LL} = 0.9$ and $m_{\text{SUSY}} = 5$ TeV, considering both the present and future LHC phases (left and right panels, respectively). On the other hand, the $h \rightarrow \tau \mu$ channel (not shown) cannot supply any significant signal at the LHC in this LL case, due to its very small branching ratios, unless extremely large total integrated luminosities were considered (larger than 500 fb^{-1}). Due to the CMS exclusion region in the $(m_A, \tan \beta)$ plane [29], it is evident that we cannot expect any LFV event from neither the $h \rightarrow \tau \mu$ channel nor the $A, H \rightarrow \tau \mu$ channels in the present phase of the LHC if the unique responsible for $\tau - \mu$ mixing is the δ_{23}^{LL} parameter and $|\delta_{23}^{LL}| < 1$. The event rates from $A, H \rightarrow \tau \mu$ for the future phase of the LHC are more promising, as shown on the right panel of Figure 6. For instance, for $m_A \simeq 450$ GeV and $\tan \beta \simeq 15$, we could expect at least 1 event, and up to 5 for larger values of m_A and values of $\tan \beta \gtrsim 50$.

Next we analyze the results for the case of LR and RL mixings in the $(m_A, \tan \beta)$ plane. Figures 7 and 8 summarize the results for the $h \rightarrow \tau \mu$ and $A \rightarrow \tau \mu$ channels, respectively, in the present and future LHC stages.

On the left panel of Figure 7, where the number of expected events from the $h \rightarrow \tau \mu$ channel in the present phase of the LHC are shown as a function of m_A and $\tan \beta$, for $m_{\text{SUSY}} = 5$ TeV and $\tilde{\delta}_{23}^{LR} = \tilde{\delta}_{23}^{RL} = 5$, we see again that the maximum allowed number of events are obtained in the low $\tan \beta$ region. Tens of events are expected, up to 50 for $\tan \beta \lesssim 3$, in all the studied m_A interval. In any case, in all the allowed region the number of predicted events are softly dependent

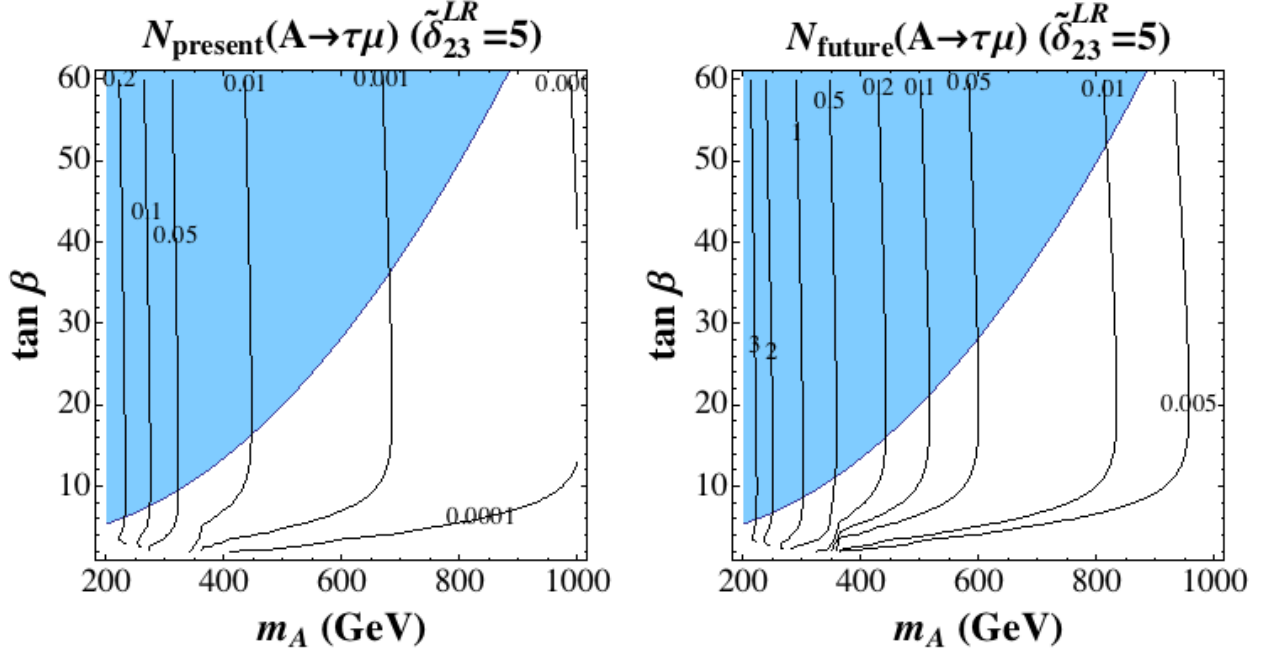


Figure 8: Number of expected LFV events in the $(m_A, \tan \beta)$ plane from $A \rightarrow \tau \mu$ for $\tilde{\delta}_{23}^{LR} = \tilde{\delta}_{23}^{RL} = 5$ and $m_{\text{SUSY}} = 5$ TeV. Left panel: present phase of the LHC with $\sqrt{s} = 8$ TeV and $\mathcal{L} = 25 \text{ fb}^{-1}$. Right panel: future phase of the LHC with $\sqrt{s} = 14$ TeV and $\mathcal{L} = 100 \text{ fb}^{-1}$. In both panels the other MSSM parameters are set to the values reported in the text, with $M_2 = m_{\text{SUSY}}$. The shaded blue areas are excluded by CMS searches [29]. The results for H (not shown) are nearly equal to these ones for A .

on m_A and at least one event is obtained, even for large values of m_A and $\tan \beta \lesssim 10$. On the right panel of Figure 7, the predictions for the $h \rightarrow \tau \mu$ channel, in the future LHC phase with a center-of-mass energy of $\sqrt{s} = 14$ TeV and a total integrated luminosity of $\mathcal{L} = 100 \text{ fb}^{-1}$, show the same behavior with respect to the two pair of parameters as on the left panel but with an increase in the number of events of around one order of magnitude. Again the maximum amount of events are for the lowest $\tan \beta$ values, being these nearly independent on m_A , and the rates decrease as we raise $\tan \beta$, showing a small variation with respect to m_A for the allowed region by data (in white), as in the previous mentioned plot. Specifically, we obtain up to 500 events for $\tan \beta \simeq 2$, and between 250 and 1 events for the region between $\tan \beta = 2$ and $\tan \beta = 35$.

The corresponding results for the $A \rightarrow \tau \mu$ channel, displayed in Figure 8, show a very different behavior with m_A and $\tan \beta$ than the previous h case. The number of expected LFV events at the LHC via $A \rightarrow \tau \mu$ decays diminish as m_A increases, due to the suppression in the production cross section of a heavy pseudoscalar Higgs boson, and stay constant with $\tan \beta$, due mainly to the compensation between the growing of the A production cross section via bottom-antibottom quark annihilation and the reduction of $\text{BR}(A \rightarrow \tau \mu)$ with this parameter, as previously illustrated in Figure 2. In the present phase of the LHC we cannot expect any event, as shown on the left panel of Figure 8. The right panel of Figure 8, containing the predictions for the $A \rightarrow \tau \mu$ channel in the future LHC phase, shows an analogous behavior to that of the left panel. The number of expected events increase around one order of magnitude respect the present LHC phase, and for values of m_A below 300 GeV, one could expect between 1 and 3 events independently on the value of $\tan \beta$.

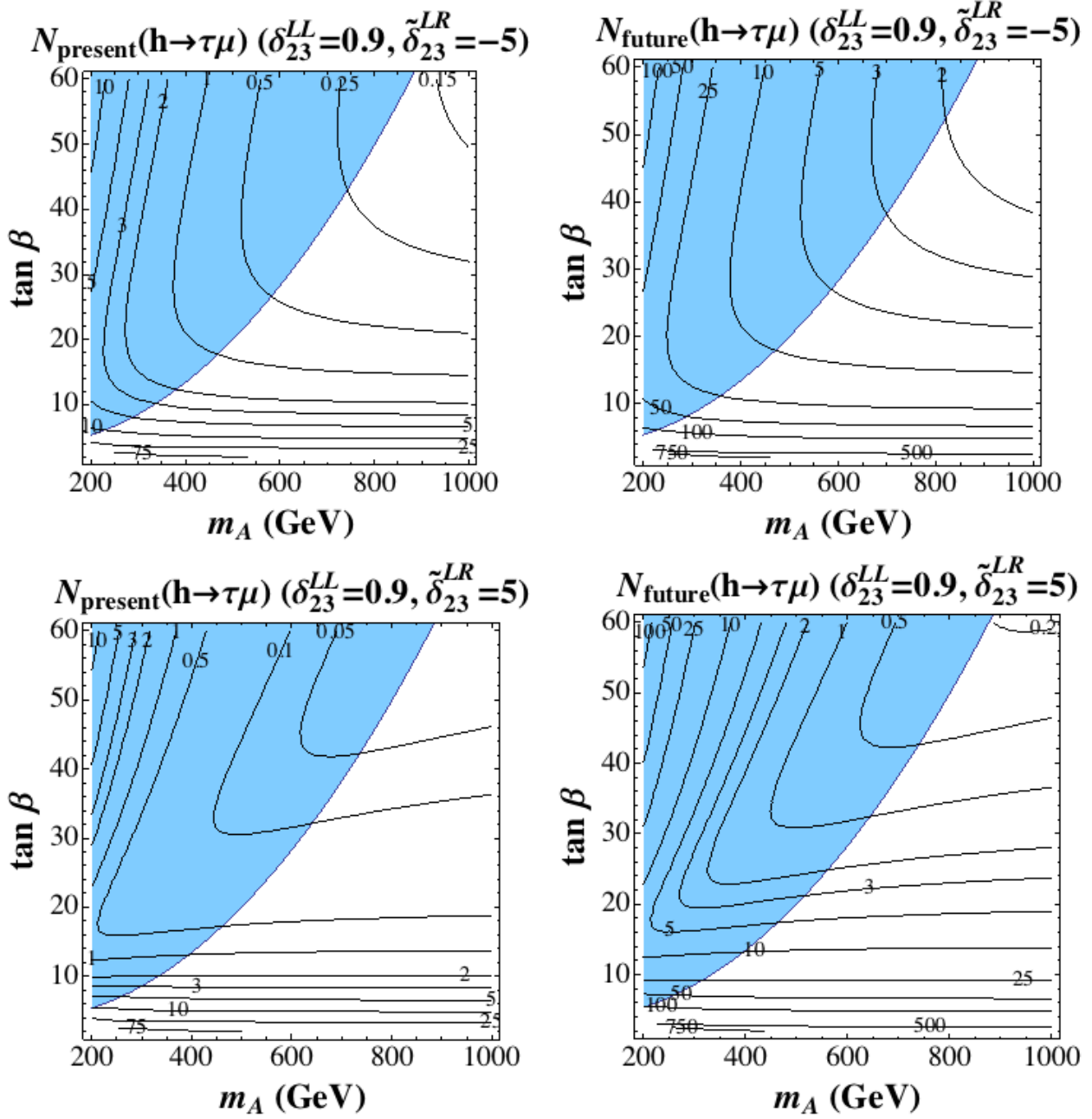


Figure 9: Number of expected LFV events in the $(m_A, \tan \beta)$ plane from $h \rightarrow \tau \mu$ for $m_{\text{SUSY}} = 5$ TeV, $\delta_{23}^{LL} = 0.9$ and $\tilde{\delta}_{23}^{LR} = \tilde{\delta}_{23}^{RL} = -5$ (upper panels) or $\tilde{\delta}_{23}^{LR} = \tilde{\delta}_{23}^{RL} = +5$ (lower panels). Left panels: present phase of the LHC with $\sqrt{s} = 8$ TeV and $\mathcal{L} = 25 \text{ fb}^{-1}$. Right panels: future phase of the LHC with $\sqrt{s} = 14$ TeV and $\mathcal{L} = 100 \text{ fb}^{-1}$. In all panels the other MSSM parameters are set to the values reported in the text, with $M_2 = m_{\text{SUSY}}$. The shaded blue areas are excluded by CMS searches [29].

Finally, the results for the $h \rightarrow \tau \mu$ and $A \rightarrow \tau \mu$ channels in the double LL and LR mixing case are summarized in Figures 9 and 10, respectively.

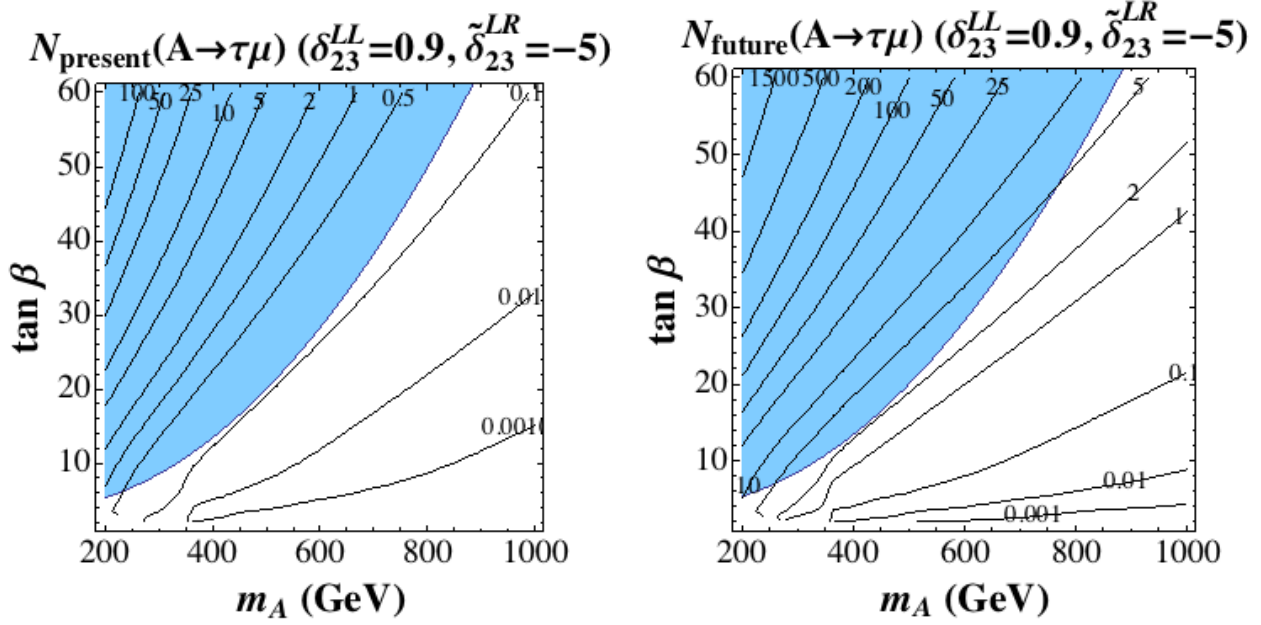


Figure 10: Number of expected LFV events in the $(m_A, \tan \beta)$ plane from $A \rightarrow \tau \mu$ for $\delta_{23}^{LL} = 0.9$, $\tilde{\delta}_{23}^{LR} = \tilde{\delta}_{23}^{RL} = -5$ and $m_{\text{SUSY}} = 5$ TeV. Left panel: present phase of the LHC with $\sqrt{s} = 8$ TeV and $\mathcal{L} = 25 \text{ fb}^{-1}$. Right panel: future phase of the LHC with $\sqrt{s} = 14$ TeV and $\mathcal{L} = 100 \text{ fb}^{-1}$. In both panels the other MSSM parameters are set to the values reported in the text, with $M_2 = m_{\text{SUSY}}$. The shaded blue areas are excluded by CMS searches [29]. The results for H (not shown) are nearly equal to these ones for A .

The predictions for the contour lines of $h \rightarrow \tau \mu$ event rates (Figure 9) show a clear different pattern than in the previous cases of single deltas. In both LHC phases, we achieve an increase in the number of events respect to the single LL and LR (and/or RL) mixing cases. The most interesting numbers are at the lower part of these plots with $\tan \beta < 10$. We find as large as 75 LFV events in the present phase of the LHC for very low values of $\tan \beta \simeq 2$ and $m_A \lesssim 600$ GeV. In the future LHC phase we predict up to 750 events, for $\tan \beta \simeq 2$ and $m_A \lesssim 450$ GeV. It should be also noted that these conclusions apply to both choices for the LR/RL mixings of -5 and $+5$, as can be seen in Figure 9. The only notable differences that we find between the results of these two cases are in the slight different patterns of the contour lines, signalling a small different sensitivity to m_A and/or $\tan \beta$. Also one can appreciate in these plots that one gets a bit lower rates for $+5$ than for -5 , in agreement with our previous findings reported in Figure 5.

The number of events for the $A \rightarrow \tau \mu$ channel in the double LL and LR mixing case are displayed in Figure 10. The LL mixing is set here to 0.9 and the $LR = RL$ mixings are fixed to -5 . As expected, the predicted event rates increase as $\tan \beta$ grows and are reduced as m_A gets bigger, due to the suppression in the production cross section of a heavy pseudoscalar Higgs boson. However, for the present LHC phase one cannot say much about this channel, since all the $m_A - \tan \beta$ regions which could produce a relevant number of LFV events are excluded at present by CMS searches. We find at the most one event in the tiny low left corner of the allowed region in this $(m_A, \tan \beta)$ plot. In contrast, the predictions in the future phase of the LHC are more promising. We predict up to about 5 LFV events for large values of m_A and $\tan \beta$ and up to 10 in the low $\tan \beta$ region with $m_A \simeq 200$ GeV. Similar conclusions are found for the case of positive

$LR=+5$ mixing (not shown). The shape of the contour lines in this case are slightly modified at low $\tan\beta$ but with no relevant implications in terms of event rates.

5 Conclusions

The discovery of a new Higgs-like particle at the LHC is concentrating a lot of efforts in studying its properties, couplings and decays, in order to investigate if there is new physics behind it. In that sense, lepton flavor violating Higgs decays are of special interest, since they would clearly imply the existence of physics beyond the SM. We have discussed in this paper the possibility of obtaining sizeable LFV Higgs rates, induced by heavy SUSY, and detectable at the LHC. In particular, we have studied in detail the most interesting LFV decays of the three neutral MSSM Higgs bosons: $h \rightarrow \tau\mu$, $H \rightarrow \tau\mu$ and $A \rightarrow \tau\mu$. We have shown that these three channels present a non-decoupling behavior with m_{SUSY} . On one hand, independently if δ_{23}^{LL} , δ_{23}^{RR} , δ_{23}^{LR} or δ_{23}^{RL} are the responsible for the intergenerational mixing in the slepton sector, these LFV Higgs decay rates remain constant with m_{SUSY} at large $m_{\text{SUSY}} > 2$ TeV. On the other hand, the related LFV radiative decay, $\tau \rightarrow \mu\gamma$, manifests a fast decoupling behavior with m_{SUSY} and its rates are very suppressed for large values of the SUSY scale. In this work, we have taken advantage of these two remarkable different behaviors with m_{SUSY} in order to reach sizeable LFV Higgs branching ratios which are yet allowed by the present $\tau \rightarrow \mu\gamma$ upper bound.

From our detailed analysis of the LFV Higgs decays, we have learned that the single $\tau - \mu$ mixing of RR type in the slepton sector cannot by itself provide sufficiently large rates which could be measurable at the LHC. The situation ameliorates slightly if we consider the single LL mixing case, with the largest rates at the large $\tan\beta$ region and amounting up to about 5 LFV events for the $H, A \rightarrow \tau\mu$ channels at the future phase of the LHC. We find that the mixing parameter δ_{23}^{LR} (and δ_{23}^{RL}) is the most relevant one and even when acting as single mixing parameter already gives rise to sizeable and allowed by data LFV Higgs-mediated event rates for sufficiently large values of $m_{\text{SUSY}} \geq 5$ TeV, where the LFV radiative $\tau \rightarrow \mu\gamma$ rates are suppressed below its present experimental upper bound. In this single LR -mixing case, we also find that the most promising channel is by far the $h \rightarrow \tau\mu$ decay for which we predict up to 50 events for low $\tan\beta$ in the present phase of the LHC. Regarding the $H, A \rightarrow \tau\mu$ channels, no events are expected in the present LHC phase if there is single LR (and/or RL) mixing. The situation improves noticeably if one considers the future phase of the LHC. In this case, with a total integrated luminosity of 100 fb^{-1} , we predict hundreds of LFV events from the lightest Higgs boson decay into $\tau\mu$, as much as 5×10^2 events for very low values of $\tan\beta$. For the LFV heavy Higgs bosons decays the expectations are lower, but also increase in comparison with the present LHC phase, and a few events could be obtained depending on the values of m_A , $\tan\beta$ and m_{SUSY} . Finally, by considering double LL and LR mixings we obtain the most interesting situation, since on one hand the rates are slightly increased with respect to the single LR mixing case and, on the other hand, the slight change in the sensitivity to $\tan\beta$ makes that larger values of this parameter than in the single LR mixing case give rise also to sizeable event rates. For instance, one can get in this double mixing case a few events at the present stage of the LHC even for moderate $\tan\beta \sim 15$ and large $m_A \geq 500$ GeV. In the future LHC phase the reach to larger $\tan\beta$ values increases and one gets some event even at very large $\tan\beta \sim 40$ and $m_A \geq 800$ GeV. The largest rates found are in any case for $h \rightarrow \tau\mu$ and are clearly localized at the low $\tan\beta$ region where we predict for the present LHC phase up to about 75 events, and up to about 750 LFV events for the future LHC phase. In the future LHC phase, we get about 10 events at the most for the $H, A \rightarrow \tau\mu$ channels in the low $\tan\beta$ region and 5 events at the most in the high $\tan\beta$ region. As a final comment, it is worth recalling that all the rates presented in this work are doubled if one adds the decay events for the two possible final

states, $\tau^+\mu^-$ and $\tau^-\mu^+$.

The encouraging results presented along this work strongly suggest that a dedicated search for the proposed LFV Higgs decays is extremely worthwhile and we believe that it should be further studied by the experiments at the LHC. If the SUSY mass scale is too heavy, as the present experiments are pointing out, and the SUSY particles cannot be directly reachable at the present or next future LHC energies, our proposal for LFV Higgs decays could provide an unique window to explore new physics and to find some hint of very heavy SUSY at the LHC.

Acknowledgments

E.A. thanks Alejandro Szynkman for fruitful discussions and a careful reading of the manuscript. M.J.H thanks Andreas Crivellin for a critical reading of a preliminary version of this paper and for some interesting comments and discussions. M.J.H also thanks Alberto Casas for his clarifying comments on the general bounds from vacuum instabilities, their domain of applicability and the way out from these bounds. The authors also thank Sven Heinemeyer for helpful information about the code `FeynHiggs`. E.A. is financially supported by a MICINN postdoctoral fellowship (Spain), under grant No. FI-2010-0041, and partially by ANPCyT (Argentina) under grant No. PICT-PRH 2009-0054 and by CONICET (Argentina) PIP-2011. E.A. thanks IFLP-CONICET for hospitality and support. The work of M.H. and M.A.-C. was partially supported by CICYT (grant FPA2009-09017), the Comunidad de Madrid project HEPHACOS, S2009/ESP-1473, the European Union FP7 ITN INVISIBLES (Marie Curie Actions, PITN-GA-2011-289442) and also by the Spanish Consolider-Ingenio 2010 Programme CPAN (CSD2007-00042).

References

- [1] M. T. Dova, *SUSY searches at LHC*, IX Latin American Symposium on High Energy Physics, SILAFAE 2012; J. Marrouche, *Search for 3rd generation and gluino induced SUSY production*, XLVIIIth Rencontres de Moriond EW 2013; M. Verducci, *Search for EWKino production and long-lived particles at the LHC*, XLVIIIth Rencontres de Moriond EW 2013; J. Maurer, *Search for supersymmetry in events with same-sign dileptons, jets and missing transverse momentum with the ATLAS detector*, XLVIIIth Rencontres de Moriond EW 2013; S. Folgueras, *Search for new physics using events with two same-sign isolated leptons in the final state*, XLVIIIth Rencontres de Moriond EW 2013; A. Favareto, *Third Generation SUSY Searches at the LHC*, XLVIIIth Rencontres de Moriond QCD 2013; A. Mann, *SUSY Searches for Inclusive Squark and Gluino Production at the LHC*, XLVIIIth Rencontres de Moriond QCD 2013; P. Everaerts, *SUSY Searches for EWK Production of Gauginos and Sleptons at the LHC*, XLVIIIth Rencontres de Moriond QCD 2013.
- [2] G. Aad *et al.* [ATLAS Collaboration], Phys. Lett. B **716** (2012) 1 [arXiv:1207.7214 [hep-ex]].
- [3] S. Chatrchyan *et al.* [CMS Collaboration], Phys. Lett. B **716** (2012) 30 [arXiv:1207.7235 [hep-ex]].
- [4] For recent works oriented to heavy SUSY searches at the LHC, see for instance: L. J. Hall, Y. Nomura and S. Shirai, JHEP **1301** (2013) 036 [arXiv:1210.2395 [hep-ph]]; J. Unwin, Phys. Rev. D **86** (2012) 095002 [arXiv:1210.4936 [hep-ph]]; E. Arganda, J. L. Diaz-Cruz and A. Szynkman, Eur. Phys. J. C **73** (2013) 2384 [arXiv:1211.0163 [hep-ph]]; N. Arkani-Hamed, A. Gupta, D. E. Kaplan, N. Weiner and T. Zorawski, arXiv:1212.6971 [hep-ph]; E. Arganda,

- J. L. Diaz-Cruz and A. Szynekman, Phys. Lett. B **722** (2013) 100 [arXiv:1301.0708 [hep-ph]]; D. McKeen, M. Pospelov and A. Ritz, arXiv:1303.1172 [hep-ph]; A. Djouadi and J. Quevillon, arXiv:1304.1787 [hep-ph].
- [5] H. E. Haber, M. J. Herrero, H. E. Logan, S. Penaranda, S. Rigolin and D. Temes, Phys. Rev. D **63** (2001) 055004 [hep-ph/0007006].
 - [6] A. Dobado, M. J. Herrero and D. Temes, Phys. Rev. D **65** (2002) 075023 [hep-ph/0107147].
 - [7] A. M. Curiel, M. J. Herrero and D. Temes, Phys. Rev. D **67** (2003) 075008 [hep-ph/0210335].
 - [8] A. M. Curiel, M. J. Herrero, W. Hollik, F. Merz and S. Penaranda, Phys. Rev. D **69** (2004) 075009 [hep-ph/0312135].
 - [9] E. Arganda, A. M. Curiel, M. J. Herrero and D. Temes, Phys. Rev. D **71** (2005) 035011 [hep-ph/0407302].
 - [10] T. Appelquist and J. Carazzone, Phys. Rev. D **11** (1975) 2856.
 - [11] E. Arganda and M. J. Herrero, Phys. Rev. D **73** (2006) 055003 [hep-ph/0510405].
 - [12] E. Arganda, M. J. Herrero and J. Portoles, JHEP **0806** (2008) 079 [arXiv:0803.2039 [hep-ph]].
 - [13] M. J. Herrero, J. Portoles and A. M. Rodriguez-Sanchez, Phys. Rev. D **80** (2009) 015023 [arXiv:0903.5151 [hep-ph]].
 - [14] E. Arganda, M. J. Herrero and A. M. Teixeira, JHEP **0710** (2007) 104 [arXiv:0707.2955 [hep-ph]].
 - [15] A. Abada, D. Das and C. Weiland, JHEP **1203** (2012) 100 [arXiv:1111.5836 [hep-ph]]; A. Abada, D. Das, A. Vicente and C. Weiland, JHEP **1209** (2012) 015 [arXiv:1206.6497 [hep-ph]].
 - [16] A. Crivellin, Phys. Rev. D **83** (2011) 056001 [arXiv:1012.4840 [hep-ph]]; A. Crivellin, L. Hofer and J. Rosiek, JHEP **1107** (2011) 017 [arXiv:1103.4272 [hep-ph]].
 - [17] N. Liu, L. Wu, P. W. Wu and J. M. Yang, JHEP **1301** (2013) 161 [arXiv:1208.3413 [hep-ph]].
 - [18] M. Raidal, A. van der Schaaf, I. Bigi, M. L. Mangano, Y. K. Semertzidis, S. Abel, S. Albino and S. Antusch *et al.*, Eur. Phys. J. C **57** (2008) 13 [arXiv:0801.1826 [hep-ph]].
 - [19] J. L. Diaz-Cruz and J. J. Toscano, Phys. Rev. D **62** (2000) 116005 [hep-ph/9910233]; J. L. Diaz-Cruz, JHEP **0305** (2003) 036 [hep-ph/0207030]; A. Brignole and A. Rossi, Phys. Lett. B **566** (2003) 217 [hep-ph/0304081]; A. Brignole and A. Rossi, Nucl. Phys. B **701** (2004) 3 [hep-ph/0404211]; S. Kanemura, K. Matsuda, T. Ota, T. Shindou, E. Takasugi, K. Tsumura and , Phys. Lett. B **599** (2004) 83 [hep-ph/0406316]; J. K. Parry, Nucl. Phys. B **760** (2007) 38 [hep-ph/0510305]; J. L. Diaz-Cruz, D. K. Ghosh and S. Moretti, Phys. Lett. B **679** (2009) 376 [arXiv:0809.5158 [hep-ph]]; P. T. Giang, L. T. Hue, D. T. Huong and H. N. Long, Nucl. Phys. B **864** (2012) 85 [arXiv:1204.2902 [hep-ph]]; A. Arhrib, Y. Cheng and O. C. W. Kong, Europhys. Lett. **101** (2013) 31003 [arXiv:1208.4669 [hep-ph]]; A. Arhrib, Y. Cheng and O. C. W. Kong, Phys. Rev. D **87** (2013) 015025 [arXiv:1210.8241 [hep-ph]].
 - [20] G. Blankenburg, J. Ellis and G. Isidori, Phys. Lett. B **712** (2012) 386 [arXiv:1202.5704 [hep-ph]].

- [21] J. Adam *et al.* [MEG Collaboration], arXiv:1303.0754 [hep-ex].
- [22] R. Harnik, J. Kopp and J. Zupan, JHEP **1303** (2013) 026 [arXiv:1209.1397 [hep-ph]]; S. Davidson and P. Verdier, Phys. Rev. D **86** (2012) 111701 [arXiv:1211.1248 [hep-ph]].
- [23] B. Aubert *et al.* [BABAR Collaboration], Phys. Rev. Lett. **104** (2010) 021802 [arXiv:0908.2381 [hep-ex]].
- [24] M. Arana-Catania, S. Heinemeyer and M. J. Herrero, Phys. Rev. D **88** (2013) 015026 [arXiv:1304.2783 [hep-ph]].
- [25] J. A. Casas and S. Dimopoulos, Phys. Lett. B **387** (1996) 107 [hep-ph/9606237].
- [26] J. -h. Park, Phys. Rev. D **83** (2011) 055015 [arXiv:1011.4939 [hep-ph]].
- [27] W. Porod, Comput. Phys. Commun. **153** (2003) 275 [hep-ph/0301101]; W. Porod and F. Staub, Comput. Phys. Commun. **183** (2012) 2458 [arXiv:1104.1573 [hep-ph]].
- [28] S. Heinemeyer, W. Hollik and G. Weiglein, Comput. Phys. Commun. **124** (2000) 76 [hep-ph/9812320]; S. Heinemeyer, W. Hollik and G. Weiglein, Eur. Phys. J. C **9** (1999) 343 [hep-ph/9812472]; G. Degrossi, S. Heinemeyer, W. Hollik, P. Slavich and G. Weiglein, Eur. Phys. J. C **28**, (2003)133 [hep-ph/0212020]; M. Frank, T. Hahn, S. Heinemeyer, W. Hollik, H. Rzehak and G. Weiglein, JHEP **0702** (2007) 047 [hep-ph/0611326].
- [29] S. Chatrchyan *et al.* [CMS Collaboration], CMS-PAS-HIG-12-050.

Erratum: Non-decoupling SUSY in LFV Higgs decays: a window to new physics at the LHC

M. ARANA-CATANIA^{1*}, E. ARGANDA^{2†}, M.J. HERRERO^{1‡}

¹*Departamento de Física Teórica and Instituto de Física Teórica, IFT-UAM/CSIC
Universidad Autónoma de Madrid, Cantoblanco, Madrid, Spain*

²*Departamento de Física Teórica, Facultad de Ciencias,
Universidad de Zaragoza, E-50009 Zaragoza, Spain*

ERRATUM TO: [JHEP09\(2013\)160](#)

ARXIV EPRINT: [1304.3371](#)

In this short note we have reviewed the numerical results of the rates for the $h, H, A \rightarrow \tau\mu$ decay channels that are originated from slepton flavor mixings of LR and RL types after correcting a detected bug in our FORTRAN code used in [1]. We have found an unfortunate missing global $1/\sqrt{2}$ factor in the contribution to the LR and RL form factors from the vertex diagram with two sleptons and one neutralino in the triangular loop, which once introduced it turns out that produces a cancellation among the dominant non-decoupling contributions, i.e. constant with the large m_{SUSY} scale, from this diagram and the external leg loop diagram with one slepton and one neutralino in the loop. These two diagrams are the dominant ones in the LR and RL cases and when added and after correcting the mentioned mistake, it results in a total decoupling behavior with the large m_{SUSY} scale instead of the total non-decoupling behavior wrongly obtained before. There is consequently a considerable reduction of all the LFV ratios if $\tilde{\delta}_{23}^{LR}$ (or $\tilde{\delta}_{23}^{RL}$) is the responsible of the flavor slepton mixing. We have redone all the plots referred to these two parameters in [1] and we present them here. The plots for the predictions of the LHC rates due to these LR and RL parameters (figures 7 and 8) are then strongly affected. We conclude here that no measurable rates can be found at the LHC if the flavor mixing between the second and the third slepton generations is of LR (or RL) type. Therefore, the results of figures 9 and 10 would be equivalent to have only $\delta_{23}^{LL} = 0.9$ as in figure 6. All the results for mixings of LL and RR types in [1] remain valid and they are not affected at all by this mistake.

*miguel.arana@uam.es

†ernesto.arganda@unizar.es

‡maria.herrero@uam.es

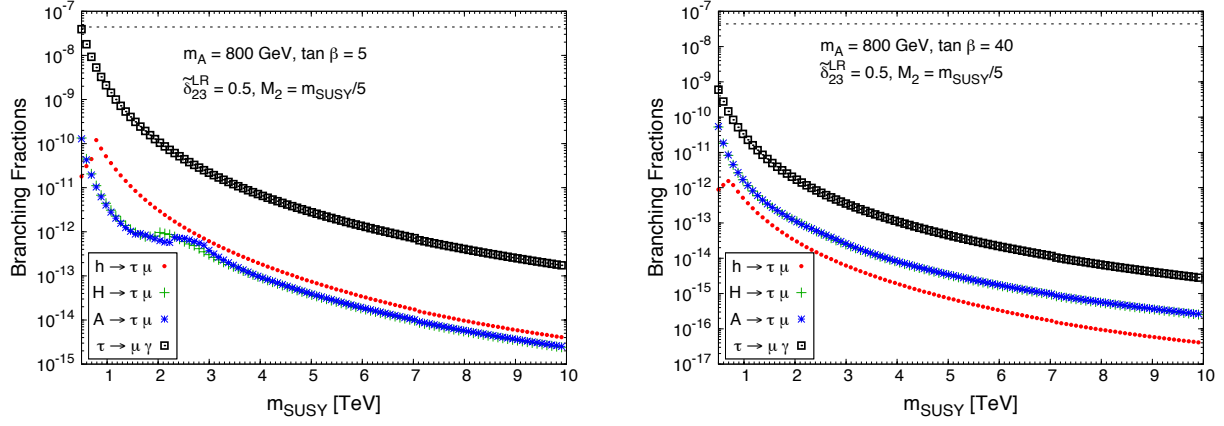


Figure 1: Large m_{SUSY} behavior of the LFV decay rates: $\text{BR}(h \rightarrow \tau\mu)$, $\text{BR}(H \rightarrow \tau\mu)$, $\text{BR}(A \rightarrow \tau\mu)$ and $\text{BR}(\tau \rightarrow \mu\gamma)$ as functions of m_{SUSY} for $\tan\beta = 5$ (left panel) and $\tan\beta = 40$ (right panel) with $\tilde{\delta}_{23}^{LR} = 0.5$. The results for $\tilde{\delta}_{23}^{RL} = 0.5$ (not shown) are identical to those of $\tilde{\delta}_{23}^{LR} = 0.5$. In each case, the other flavor changing deltas are set to zero. In all panels, $m_A = 800$ GeV and the other MSSM parameters are set to the values reported in the text, with $M_2 = \frac{1}{5}m_{\text{SUSY}}$. The horizontal dashed line denotes the current experimental upper bound for $\tau \rightarrow \mu\gamma$ channel, $\text{BR}(\tau \rightarrow \mu\gamma) < 4.4 \times 10^{-8}$.

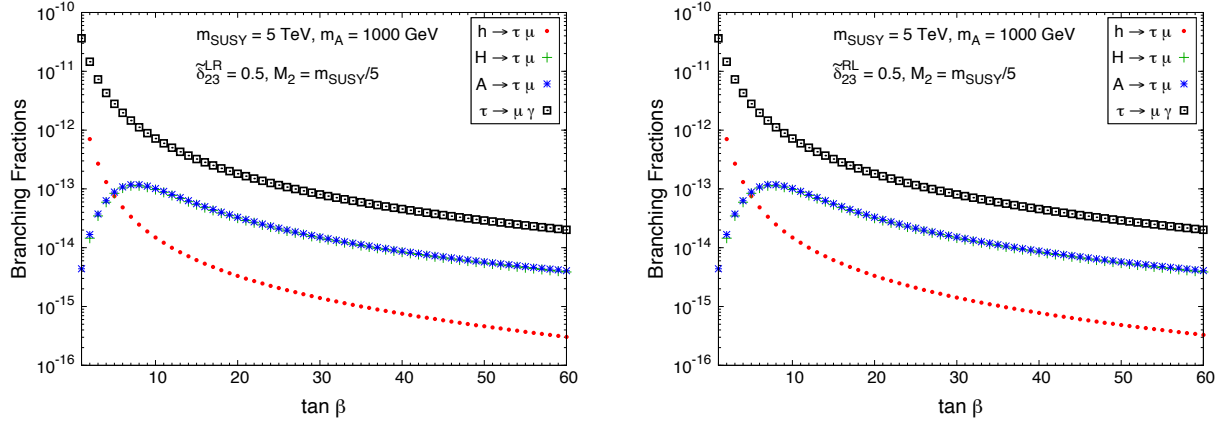


Figure 2: $\text{BR}(h \rightarrow \tau\mu)$, $\text{BR}(H \rightarrow \tau\mu)$, $\text{BR}(A \rightarrow \tau\mu)$ and $\text{BR}(\tau \rightarrow \mu\gamma)$ as functions of $\tan\beta$ for $\tilde{\delta}_{23}^{LR} = 0.5$ (left panel) and $\tilde{\delta}_{23}^{RL} = 0.5$ (right panel). In each case, the other flavor changing deltas are set to zero. In all panels, $m_A = 1000$ GeV, $m_{\text{SUSY}} = 5$ TeV and the other MSSM parameters are set to the values reported in the text, with $M_2 = m_{\text{SUSY}}/5$.

Acknowledgments

We wish to thank Andreas Crivellin for his several remarks and discussions on our first (wrong) results for these LR and RL cases which were not showing the decoupling behavior that he was expecting. Our corrected results included here manifest clearly this expected decoupling behavior with the SUSY mass scale m_{SUSY} .

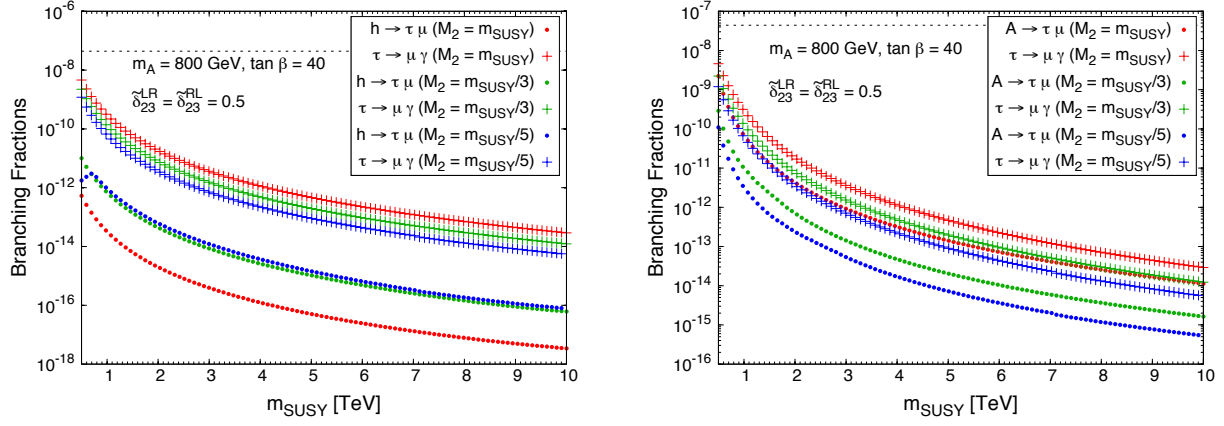


Figure 3: Sensitivity to M_2 : LFV Higgs decay rates (dots) and $\text{BR}(\tau \rightarrow \mu\gamma)$ (crosses) as functions of m_{SUSY} with $\tilde{\delta}_{23}^{LR} = \tilde{\delta}_{23}^{RL} = 0.5$ for different choices of M_2 : $M_2 = m_{\text{SUSY}}$ (in red), $M_2 = \frac{1}{3}m_{\text{SUSY}}$ (in green) and $M_2 = \frac{1}{5}m_{\text{SUSY}}$ (in blue). The results for H (not shown) are nearly identical to those of A . In each case, the other flavor changing deltas are set to zero. In all panels, $m_A = 800$ GeV, $\tan\beta = 40$ and the other MSSM parameters are set to the values reported in the text. The horizontal dashed line denotes the current experimental upper bound for $\tau \rightarrow \mu\gamma$ channel, $\text{BR}(\tau \rightarrow \mu\gamma) < 4.4 \times 10^{-8}$.

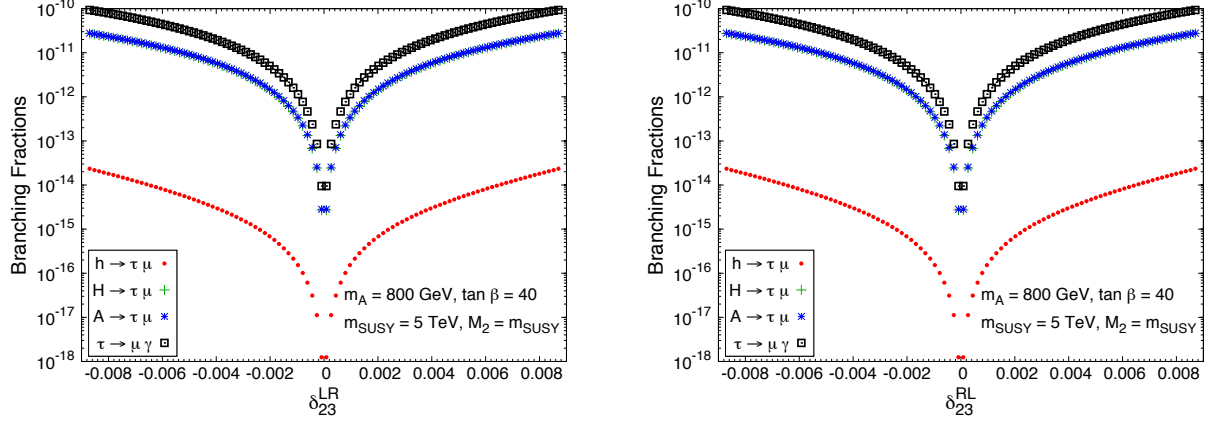


Figure 4: $\text{BR}(h \rightarrow \tau\mu)$, $\text{BR}(H \rightarrow \tau\mu)$, $\text{BR}(A \rightarrow \tau\mu)$ and $\text{BR}(\tau \rightarrow \mu\gamma)$ as functions of δ_{23}^{LR} (left panel) and δ_{23}^{RL} (right panel). In each case, the other flavor changing deltas are set to zero. In all panels, $m_A = 800$ GeV, $\tan\beta = 40$, $m_{\text{SUSY}} = 5$ TeV and the other MSSM parameters are set to the values reported in the text, with $M_2 = m_{\text{SUSY}}$.

References

- [1] M. Arana-Catania, E. Arganda and M. J. Herrero, JHEP **1309** (2013) 160 [arXiv:1304.3371 [hep-ph]].

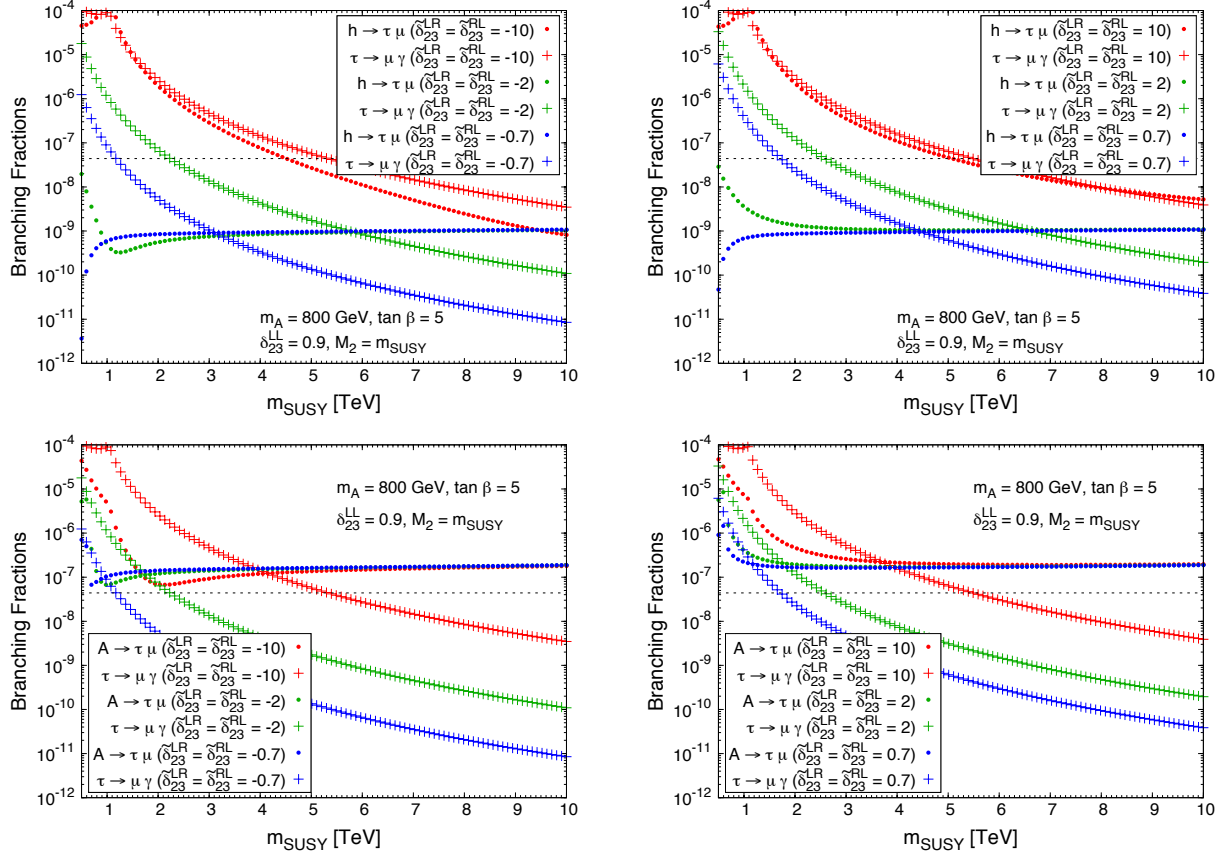


Figure 5: Sensitivity to double LL and LR mixing deltas: LFV Higgs decay rates (dots) and $\text{BR}(\tau \rightarrow \mu\gamma)$ (crosses) as functions of m_{SUSY} with $\delta_{23}^{LL} = 0.9$ for different choices of negative LR mixing (left panels), $\tilde{\delta}_{23}^{LR} = \tilde{\delta}_{23}^{RL}$: -0.7 (in blue), -2 (in green) and -10 (in red), and of positive LR mixing (right panels), $\tilde{\delta}_{23}^{LR} = \tilde{\delta}_{23}^{RL}$: +0.7 (in blue), +2 (in green) and +10 (in red). The results for H (not shown) are nearly identical to those of A . In each case, the other flavor changing deltas are set to zero. In both panels, $m_A = 800$ GeV, $\tan \beta = 5$, $M_2 = m_{\text{SUSY}}$ and the other MSSM parameters are set to the values reported in the text. The horizontal dashed line denotes the current experimental upper bound for $\tau \rightarrow \mu\gamma$ channel, $\text{BR}(\tau \rightarrow \mu\gamma) < 4.4 \times 10^{-8}$.